

## Influence of chiral chemical potential $\mu_5$ on phase structure of the two-color quark matter

T. G. Khunjua<sup>1</sup>, K. G. Klimenko<sup>2</sup>, and R. N. Zhokhov<sup>3</sup>

<sup>1</sup>*The University of Georgia, GE-0171 Tbilisi, Georgia*

<sup>2</sup>*State Research Center of Russian Federation—Institute for High Energy Physics, NRC “Kurchatov Institute”, 142281 Protvino, Moscow Region, Russia*

<sup>3</sup>*Pushkov Institute of Terrestrial Magnetism, Ionosphere and Radiowave Propagation (IZMIRAN), 108840 Troitsk, Moscow, Russia*



(Received 3 May 2022; accepted 24 July 2022; published 8 August 2022)

In this paper the influence of chiral chemical potential  $\mu_5$  on the phenomenon of diquark condensation and phase structure of dense quark matter altogether is contemplated in the framework of the effective 2-color and 2-flavor Nambu–Jona-Lasinio model. The nonzero values of baryon  $\mu_B$ , isospin  $\mu_I$  and chiral isospin  $\mu_{I5}$  chemical potentials are also taken into account. We show that the duality relations between diquark condensation, charged pion condensation, and chiral symmetry breaking phenomena, found in the case of zero  $\mu_5$ , are also valid for any value of  $\mu_5 \neq 0$ . In terms of dualities and the influence on the phase diagram, chiral imbalance  $\mu_5$  stands alone from other chemical potentials. Indeed, in comparison with other chemical potentials,  $\mu_5$  has two interesting features. (i) In the region of moderate values of  $\mu_B$ ,  $\mu_I$ , and  $\mu_{I5}$  it manifests itself as a *universal catalyst*, since it enhances just the phase that is realized in the system at  $\mu_5 = 0$ . (ii) In the second regime, when several other chemical potentials reach rather large values, one could observe a rather complicated and rich phase structure, and chiral chemical potential  $\mu_5$  can be a factor that not so much catalyzes as *triggers* rather peculiar phases.

DOI: [10.1103/PhysRevD.106.045008](https://doi.org/10.1103/PhysRevD.106.045008)

### I. INTRODUCTION

It is well known that quantum chromodynamics (QCD) is the theory of hot and dense strongly interacting matter. And the great interest are properties and phase diagram of dense baryon (quark) matter, which may be realized in heavy-ion collision experiments or inside compact stars [1]. However, at the corresponding values of temperature and baryon density, the QCD interaction constant is quite large. Therefore, using the usual perturbation method, it is impossible to obtain an adequate picture of the phenomena of dense quark matter. In this case different effective low-energy QCD-like models, among which are the well-known Nambu–Jona-Lasinio (NJL) type models [2–4], etc, can be used to describe the corresponding parts of the QCD phase diagram. Alternatively, one can apply numerical lattice Monte Carlo simulation methods (see, e.g., Ref. [5]). But due to a notorious sign problem of the quark determinant, the first-principle lattice approach in the three-color QCD is limited by the systems with zero

baryon chemical potential  $\mu_B$ , i.e., when baryon density of the system is equal to zero.<sup>1</sup>

In contrast, in the QCD with an even flavor number  $N_f$  (below we consider the two-flavor case, i.e.,  $N_f = 2$ ) of two-colored quarks the sign problem of the quark determinant is absent at  $\mu_B \neq 0$ . Moreover, this theory shares such an important aspect of real ( $N_c = 3$ )-color QCD as spontaneous chiral symmetry breaking at low temperatures. Or the low-energy excitations in both theories consist of color-singlet hadrons, etc., i.e., the 2-color QCD is a good basis to test various ideas of the 3-color QCD at  $\mu_B \neq 0$ . So a lot of investigations of the phase diagram of two-color QCD have been carried out at  $\mu_B \neq 0$  both using the lattice approach and within the framework of some low-energy effective models [6–21]. However, for the sake of clarity, it should be noted that there are serious qualitative differences between two- and three-color QCD. Namely, in the first case baryons, including diquarks, are bosons, while at  $N_c = 3$  all baryons are fermions. In addition, in the massless case the flavor (chiral) symmetry of the 3-color QCD is  $SU(N_f)_L \times SU(N_f)_R \times U(1)$ , whereas

*Published by the American Physical Society under the terms of the Creative Commons Attribution 4.0 International license. Further distribution of this work must maintain attribution to the author(s) and the published article's title, journal citation, and DOI. Funded by SCOAP<sup>3</sup>.*

<sup>1</sup>Note that throughout the paper we deal only with quarks belonging to the fundamental representation of the color  $SU(N_c)$  group. If they are in the adjoint representation of the  $SU(N_c = 3)$ , then the sign problem is absent [6].

in the 2-color massless QCD this flavor symmetry is enhanced to  $SU(2N_f)$ , and sometimes referred to as the Pauli-Gursey symmetry [7]. Moreover, as it was recently shown in Ref. [22], the Standard Model based on two-color QCD can have quite different properties than at  $N_c = 3$ , etc.

Strictly speaking, all of the above refers to the description of the properties of hypothetical quark matter, which is characterized by only one, baryonic, chemical potential  $\mu_B$ . However, dense baryonic matter, which can exist in neutron stars or be even observed in heavy-ion collision experiments, is characterized by at least one more property. It is isospin asymmetry, i.e., when there are different densities of  $u$  and  $d$  quarks in medium. And in this case there appears an additional isospin chemical potential  $\mu_I$  in the system (see, e.g., the review [4]).

Moreover, in hot and magnetized quark matter chiral asymmetry of the medium can also be observed. In the most general case this phenomenon can be described by two chemical potentials, chiral  $\mu_5$  and chiral isospin  $\mu_{I5}$ , and they are thermodynamically conjugated to chiral  $n_5$  and chiral isospin  $n_{I5}$  densities, respectively (a more detailed discussion of these quantities is given in the next section). Chiral density  $n_5 = n_R - n_L$  (here  $n_R$  and  $n_L$  are densities of all right- and left-handed quarks, respectively) can be generated dynamically at high temperatures, for example, in the fireball after heavy ion collision, by virtue of the Adler-Bell-Jackiw anomaly and quarks interacting with gauge (gluon) field configurations with nontrivial topology, named sphalerons. In addition, in the presence of an external strong magnetic field  $\mathbf{B}$ , both chiral density  $n_5$  and chiral chemical potential  $\mu_5$  can be produced (even at rather low temperature) in dense quark matter due to the so-called chiral separation effect [23]. Then, it was shown that at  $\mathbf{B} \neq \mathbf{0}$  the presence of nonzero  $\mu_5$  can lead to the so-called chiral magnetic effect [24–26], i.e., when in the system of massless fermions an electric current  $\mathbf{J} \sim \mu_5 \mathbf{B}$  appears. Moreover, chiral asymmetry with  $\mu_5 \neq 0$  and chiral magnetic effect play a significant role in different physical systems such as quark-gluon plasma, chiral materials, etc. [27,28].

Usually, when we talk about chiral density  $n_5$  of the whole system (consisting of  $u$  and  $d$  quarks) one implies that chiral density  $n_{u5}$  of  $u$  quarks and chiral density  $n_{d5}$  of  $d$  quarks are equal to each other (it is evident that  $n_5 = n_{u5} + n_{d5}$ ). Indeed, that is the case when one has in mind the mechanism of generation of chiral imbalance at high temperatures due to nontrivial topology of gauge field configuration. In this case it is quite plausible that  $n_{u5} = n_{d5}$  due to the fact that gluon field interacts with different quark flavors in exactly the same way and does not feel the difference between flavors. But another mechanism, the chiral separation effect, is sensitive to the flavor of quarks (as it was shown in Appendices A to the papers [29]). So in dense quark matter (even at low temperatures) a strong magnetic field separates  $u$  and  $d$  quarks in different ways. As a result, we see that, e.g., in such astrophysical objects

as magnetars there might exist areas, in which the quantity  $n_{I5} \equiv n_{u5} - n_{d5}$ , called the chiral isospin density, is not zero. As a result, in order to study properties of the system in this case the isospin chemical potential  $\mu_{I5}$  should also be introduced.

Thus, the phase structure of real dense quark (baryonic) matter should be described, strictly speaking, in terms of QCD with several chemical potentials. But in this case, we still have no reliable first-principle computations for finite-density QCD both in the three and two-color quark approaches. The reason again lies in the sign problem of the quark determinant, which arises in the lattice approach even in the framework of the 2-color QCD when describing dense quark matter with additional chemical potentials.<sup>2</sup> And, therefore, in this case the properties of dense baryonic medium, formed from both 3-color and hypothetical 2-color quarks, are most adequately described only within the framework of low-energy effective models such as NJL models, etc.

Recently, the properties of  $N_c = 3$  dense quark matter with isospin asymmetry ( $\mu_I \neq 0$ ) have been studied just in the framework of various NJL-type models with two quark flavors, where, in particular, it was noted that at  $\mu_I > m_\pi$  (here  $m_\pi$  is the pion mass) in such a medium a phase with condensation of charged pions can be observed (for it we use the notation charged PC phase) [30–36]. Furthermore, if in addition the chiral asymmetry of quark matter is also taken into account, i.e.,  $\mu_5 \neq 0$  or  $\mu_{I5} \neq 0$ , then the possibility of appearance of the charged PC phenomenon in the system is predicted with even greater reliability [29,37–39]. Notice that in the last papers it was also shown that at  $\mu_I \neq 0$  and  $\mu_{I5} \neq 0$ , as well as at  $\mu_B \neq 0$ , there is a duality between the phenomena of spontaneous chiral symmetry breaking (CSB) and condensation of charged pions. It means that on the  $(\mu_B, \mu_I, \mu_{I5})$ -phase diagram of quark matter,<sup>3</sup> obtained in the framework of these simplest  $N_c = 3$  NJL models, (i) only nontrivial CSB and charged PC phases are present, and (ii) these phases are arranged symmetrically on the full phase portrait of quark matter (at zero bare quark mass  $m_0$  the dual symmetry is exact, but if  $m_0 \neq 0$  it is an approximate one [29]). However, since only the simplest, quark-antiquark, of all possible quark interaction channels was taken into account in the structure of these  $N_c = 3$  NJL models, the results of Refs. [29,37–39] can be trusted in the region of rather low values of baryon densities, i.e., at  $\mu_B < 1$  GeV, where other phenomena such as color superconductivity, etc are forbidden. And this is despite the fact that the above mentioned dual symmetry (property) of quark matter at low baryon densities is consistent with calculations, for example, of the

<sup>2</sup>For example, it is shown in Ref. [21] that the 2-color QCD suffers from the sign problem if both  $\mu_B$  and  $\mu_I$  are present.

<sup>3</sup>Here and below we discuss the properties of dense quark matter formed of  $u$  and  $d$  quark flavors only.

(pseudo)-critical temperature of its crossover transition to the quark gluon plasma phase, made in the lattice approach (see, e.g., the discussion in Ref. [29]). At higher densities, i.e., at  $\mu_B > 1$  GeV, in addition to the quark-antiquark, it is necessary to take into account other, for example, diquark, etc, interaction channels, which also participate in the formation of the phase portrait of dense baryonic matter.

In the present paper, an attempt is performed to find out how the phenomenon of condensation of diquark pairs, which in the real 3-color case corresponds to color superconductivity (CSC) phenomenon, can affect the duality between the CSB and charged PC phases. According to a number of studies of CSC [40], this phase of dense quark matter can be realized in the cores of neutron stars. Naturally, in this case there is an isospin asymmetry (different densities of  $u$  and  $d$  quarks) of quark matter. Moreover, it is also under the influence of strong magnetic field, leading to chiral asymmetry of quark medium (see, e.g., the discussion in Ref. [29]). To simplify the consideration of the problem, in our recent paper [41] the phase structure of the 2-color and 2-flavor massless NJL model was investigated in the mean-field approximation at three nonzero chemical potentials,  $\mu_B \neq 0$ ,  $\mu_I \neq 0$ , and  $\mu_{I5} \neq 0$ . It is well known that at low energies this model is equivalent to the 2-color QCD (see, e.g., Ref. [8]) with the same set of chemical potentials, and its simplest particle excitations are  $\sigma$  and  $\pi$  mesons and colorless diquark baryons with zero spin. So, in the ground state of the  $N_c = 2$  system under consideration there can be a condensation of  $\sigma$  particles, and in this case the CSB phase is realized. If  $\pi^\pm$  are condensed—the charged PC phase is observed. Finally, the condensation of baryonic colorless diquarks leads to the phase of quark matter with spontaneous breaking of baryonic  $U(1)_B$  symmetry, and we call it the baryonic superfluid (BSF) phase. It is shown in Ref. [41] that one more, diquark, channel of quark interactions does not spoil at all the dual symmetry between CSB and charged PC phenomena at large  $\mu_B$ . Moreover, in this case there appear two additional dual symmetries of the  $(\mu_B, \mu_I, \mu_{I5})$ -phase portrait of the model: between the BSF and CSB phases, as well as between the BSF and charged PC phases.

We emphasize once again that in the paper [41] the chiral asymmetry of 2-color quark matter was taken into account in the form when only  $\mu_{I5}$  is not equal to zero. However, in real systems the chiral asymmetry of the medium in the form when  $\mu_5 \neq 0$  could play a key role [42–46]. And in all scenarios where the chiral isospin  $\mu_{I5}$  imbalance occurs, as a rule, the chiral  $\mu_5$  imbalance is also nonzero. Furthermore, in heavy-ion collisions due to large temperatures and nontrivial gluon configurations chiral imbalance  $\mu_5$  may appear. Therefore, it would be interesting to clarify the situation with the dual symmetries of the phase diagram of this system in the most general case, when all four chemical potentials are taken into account, i.e., at  $\mu_B \neq 0$ ,  $\mu_I \neq 0$ ,  $\mu_{I5} \neq 0$ , and  $\mu_5 \neq 0$ . And clarify if chiral imbalance  $\mu_5$  breaks the dualities and how it fits in the duality picture. Moreover,

the purpose of the present paper is to investigate the influence of  $\mu_5$  on the phenomenon of diquark condensation. So the present paper is really a continuation of our previous study [41] of the properties of the 2-color NJL model. And this time we are just considering its phase structure taking into account  $\mu_5$  in addition to  $\mu_B$ ,  $\mu_I$ , and  $\mu_{I5}$ .

Let us also note that in the 2-color case one can study on lattice as nonzero  $\mu_B \neq 0$  as well as nonzero chiral imbalance  $\mu_5$  of quark matter. Hence it is of special interest to compare lattice approach to 2-color quark matter with the results obtained in effective model discussed here.

The main results and the structure of the paper are as follows. In Sec. II the 2-color NJL model and its thermodynamic potential are presented in the mean-field approximation. In Sec. III the thermodynamic potential is calculated and it is shown that three dualities found in the case  $\mu_5 = 0$  in Ref. [41] are also valid in the general case at any  $\mu_5 \neq 0$ . It turns out that the full  $(\mu_B, \mu_I, \mu_{I5}, \mu_5)$ -phase diagram of the model is interconnected by the dualities and possesses a very high (dual) symmetry. Chiral  $\mu_5$  is the only chemical potential that keeps the dual symmetry intact but is not involved in it itself, it only deforms the whole phase diagram. This deformation should respect the high symmetry that puts rather tight constraints on the possible influence of  $\mu_5$  on the phase diagram.

In Sec. IV the phase diagram itself is studied numerically. Section IV A contains the discussion of the case when besides  $\mu_5 \neq 0$ , only one of the basic chemical potentials  $\mu_B$ ,  $\mu_I$  and  $\mu_{I5}$  is nonzero. Already in this case, one could see two interesting features of chiral  $\mu_5$  imbalance, its chameleon nature and its property of being universal catalyst. It is shown that it can catalyze every phenomena in the system: the catalysis of CSB by  $\mu_5$  was discussed in detail in the literature before (see, e.g., in Refs. [46–48]), but the catalysis/enhancement of charged PC and diquark condensation by chiral  $\mu_5$  imbalance is its new feature. Chameleon nature signifies that chiral  $\mu_5$  chemical potential can take on a role of any other chemical potential and have the same influence on the phase structure (being universal catalyzer is one of manifestations of chameleon properties). In particular, chiral chemical potential can take a role of isospin one and in equal degree catalyze charged PC, or it can mimic baryon one and catalyze diquark condensation. These properties are implications of high symmetry of the phase diagram that is caused by duality properties.

In Sec. IV B the regime of small or moderate values of the basic chemical potentials  $\mu_B$ ,  $\mu_I$ , and  $\mu_{I5}$  is discussed. One should not treat this regime as only small values of these chemical potentials and it covers quite a bit of the phase diagram just excluding the regime when several, two or three, chemical potentials  $\mu_B$ ,  $\mu_I$ , and  $\mu_{I5}$  reach high values. In this regime the phase diagram is very concise and elegant, each of the basic chemical potential triplet supports only one specific phenomenon ( $\mu_{I5}$  induces chiral symmetry breaking,  $\mu_I$ —charged PC and  $\mu_B$  leads to diquark condensation), and the

largest of the basic chemical potential settles the corresponding phase. In this regime,  $\mu_5$  does not break this correspondence and does not play any role in determining the prevailed phase, but its role is the same as in particular case discussed above, i.e., in Sec. IV A, it is universal catalyzer which *enhances/catalyzes* all the phenomena picked by other chemical potentials on equal footing.

Section IV C contains the consideration of the regime when several, two or three, basic chemical potentials reach rather high values. In Sec. IV C 1 we study the case when only two of chemical potentials  $\mu_B$ ,  $\mu_I$ , and  $\mu_{I5}$  are large and nonzero. In this case  $\mu_5$  can cause nontrivial phases to appear, and, depending on the conditions, as a chameleon it could mimic various chemical potentials and *trigger* all the possible phases. Section IV C 2 contains the discussion of the most generic case when all basic chemical potentials are nonzero. One could observe a rather complicated and rich phase structure in this case and chiral  $\mu_5$  chemical potential is shown to *trigger* rather peculiar phases. For example, diquark condensation by taking the role of baryon chemical potential (at zero baryon chemical potential), which is quite unusual. Or charged PC at  $\mu_I = 0$  by mimicking the property of isospin chemical potential, etc. Also the transitory regime is considered, i.e., borderline region between the discussed above regimes. In this case especially rich phase structure is observed and by changing chemical potentials in a rather narrow range a series of first order phase transitions between all the possible phases of the system could be observed.

## II. TWO-COLOR (3+1)-DIMENSIONAL NJL MODEL AND ITS THERMODYNAMIC POTENTIAL

In order to obtain an effective 4-quark Lagrangian (which is usually called the NJL Lagrangian) that would reproduce the basic low-energy properties of dense quark matter with isospin and chiral asymmetries and formed by  $u$  and  $d$  two-color quarks, it is necessary first to integrate out the gluon fields in the generating functional of the corresponding QCD theory. Then, replacing the nonperturbative gluon propagator by a  $\delta$ -function, one arrives at an effective local chiral four-quark interaction Lagrangian of the form (color current)  $\times$  (color current) of the NJL type describing low-energy hadron physics. Finally, by performing a Fierz transformation of this interaction term and taking into account only scalar and pseudoscalar ( $\bar{q}q$ )—as well as scalar ( $qq$ )-interaction channels, one obtains a four-fermionic model given by the following Lagrangian (in Minkowski space-time notation)<sup>4</sup>

$$L = \bar{q}[i\hat{\partial} - m_0]q + H[(\bar{q}q)^2 + (\bar{q}i\gamma^5\vec{\tau}q)^2 + (\bar{q}i\gamma^5\sigma_2\tau_2q^c)(\overline{q^c}i\gamma^5\sigma_2\tau_2q)] + \bar{q}\mathcal{M}\gamma^0q, \quad (1)$$

where (here we use the notations  $\mu = \mu_B/2$ ,  $\nu = \mu_I/2$ , and  $\nu_5 = \mu_{I5}/2$ )<sup>5</sup>

$$\mathcal{M} = \mu + \nu\tau_3 + \nu_5\gamma^5\tau_3 + \mu_5\gamma^5. \quad (2)$$

In (1), the quark field  $q \equiv q_{i\alpha}$  is a flavor and color doublet as well as a four-component Dirac spinor, where  $i = 1, 2$  or  $u, d$ ;  $\alpha = 1, 2$ . (Latin and Greek indices refer to flavor and color indices, respectively; spinor indices are omitted.) Furthermore, we use the notations  $\vec{\tau} \equiv (\tau_1, \tau_2, \tau_3)$  and  $\sigma_2$  for usual Pauli matrices acting in the two-dimensional flavor and color spaces, respectively;  $\hat{\partial} \equiv \gamma^\rho\partial_\rho$ ;  $q^c = C\bar{q}^T$ ,  $\overline{q^c} = q^TC$  are charge-conjugated spinors, and  $C = i\gamma^2\gamma^0$  is the charge conjugation matrix (the symbol  $T$  denotes the transposition operation). The Lagrangian (1) is invariant with respect to color  $SU(2)_c$  and baryon  $U(1)_B$  symmetries. Moreover, in the chiral limit,  $m_0 = 0$ , and at zero values of all chemical potentials it has the same Pauli-Gursey flavor  $SU(4)$  symmetry as the corresponding two-color QCD.

The Lagrangian  $L$  of Eq. (1) contains baryon  $\mu_B$ , isospin  $\mu_I$ , chiral isospin  $\mu_{I5}$ , and chiral  $\mu_5$  chemical potentials. In other words, this model is able to describe the properties of quark matter with nonzero baryon  $n_B = (n_u + n_d)/2 \equiv n/2$ , isospin  $n_I = (n_u - n_d)/2$ , chiral isospin  $n_{I5} = (n_{u5} - n_{d5})/2$ , and chiral  $n_5 = n_R - n_L$  densities which are the quantities, thermodynamically conjugated to chemical potentials  $\mu_B$ ,  $\mu_I$ ,  $\mu_{I5}$ , and  $\mu_5$ , respectively. (Here we use the notations  $n_f$  and  $n_{fL(R)}$  for density of quarks as well as density of left (right)-handed quarks,  $q_{L/R} = \frac{1 \mp \gamma^5}{2}q$ , with individual flavor  $f = u, d$ , respectively. Moreover,  $n_{f5} = n_{fR} - n_{fL}$  and  $n_{R(L)} = n_{uR(L)} + n_{dR(L)}$ . It is also supposed throughout the paper that quark fields in Eq. (1) have a baryon charge equal to  $1/2$ .) Below we need the expressions for the chemical potentials  $\mu_{fL(R)}$ , i.e., quantities which are thermodynamically conjugated to the particle number densities  $n_{fL(R)}$  of left-handed (right-handed)  $f = u, d$  quarks, respectively,

$$\begin{aligned} \mu_{uL} &= \mu + \nu + \mu_5 + \nu_5, & \mu_{uR} &= \mu + \nu - \mu_5 - \nu_5, \\ \mu_{dL} &= \mu - \nu + \mu_5 - \nu_5, & \mu_{dR} &= \mu - \nu - \mu_5 + \nu_5. \end{aligned} \quad (3)$$

The quantities (3) can be obtained from Eqs. (1) and (2). They define Fermi energies for massless  $u_{L(R)}$  and  $d_{L(R)}$

<sup>4</sup>The most general Fierz transformed four-fermion interaction includes additional vector and axial-vector ( $\bar{q}q$ ) as well as pseudoscalar, vector and axial-vector-like ( $qq$ )-interactions. However, these terms are omitted here for simplicity.

<sup>5</sup>Do not be confused, but below for the values of  $\mu$ ,  $\nu$ , and  $\nu_5$  we will usually use the names baryon, isospin, and chiral isospin chemical potentials, respectively.

quarks. Note that at  $m_0 = 0$  the Lagrangian (1) is no longer invariant with respect to Pauli-Gursey  $SU(4)$  symmetry. Due to the terms with chemical potentials, this symmetry is reduced to the Abelian  $U(1)_B$ ,  $U(1)_{I_3}$  and  $U(1)_{A_{I_3}}$  groups, where

$$\begin{aligned} U(1)_B: q &\rightarrow \exp(i\alpha/2)q; & U(1)_{I_3}: q &\rightarrow \exp(i\alpha\tau_3/2)q; \\ U(1)_{A_{I_3}}: q &\rightarrow \exp(i\alpha\gamma^5\tau_3/2)q. \end{aligned} \quad (4)$$

Moreover, the quantities  $n_B$ ,  $n_I$ , and  $n_{I_5}$  are the ground state expectation values of the densities of conserved charges corresponding to  $U(1)_B$ ,  $U(1)_{I_3}$  and  $U(1)_{A_{I_3}}$  symmetry groups. So we have from (4) that  $n_B = \langle \bar{q}\gamma^0 q \rangle / 2$ ,  $n_I = \langle \bar{q}\gamma^0 \tau^3 q \rangle / 2$  and  $n_{I_5} = \langle \bar{q}\gamma^0 \gamma^5 \tau^3 q \rangle / 2$ . However, the chiral chemical potential  $\mu_5$  does not correspond to a conserved quantity of the model (1). It is usually introduced in order to describe a system on the timescales when all chirality changing processes are finished in the system, so it is in the state of thermodynamical equilibrium with some fixed value of the chiral density  $n_5$  [43,44]. The ground state expectation values of  $n_B$ ,  $n_I$ ,  $n_{I_5}$ , and  $n_5$  can be found by differentiating the thermodynamic potential (TDP) of the system (1) with respect to the corresponding chemical potentials. The goal of the present paper is the investigation of the ground state properties (or phase structure) of the NJL model (1) and its dependence on the chemical potentials  $\mu_B$ ,  $\mu_I$ ,  $\mu_{I_5}$ , and  $\mu_5$ .

To find the TDP, we starting from a semibosonized (linearized) version of the Lagrangian (1) that contains auxiliary bosonic fields  $\sigma(x)$ ,  $\vec{\pi} = (\pi_1(x), \pi_2(x), \pi_3(x))$ ,  $\Delta(x)$  and  $\Delta^*(x)$  and has the following form

$$\begin{aligned} \tilde{L} = & \bar{q}[i\hat{d} - m_0 + \mathcal{M}\gamma^0 - \sigma - i\gamma^5 \vec{\tau} \vec{\pi}]q - \frac{\sigma^2 + \vec{\pi}^2 + \Delta^* \Delta}{4H} \\ & - \frac{\Delta}{2} [\bar{q}i\gamma^5 \sigma_2 \tau_2 q^c] - \frac{\Delta^*}{2} [\bar{q}^c i\gamma^5 \sigma_2 \tau_2 q], \end{aligned} \quad (5)$$

where  $\mathcal{M}$  is presented in Eq. (2). Clearly, the Lagrangians (1) and (5) are equivalent, as can be seen by using the Euler-Lagrange equations of motion for bosonic fields which take the form

$$Z = \begin{pmatrix} D^+ & K \\ K^* & D^- \end{pmatrix} \equiv \begin{pmatrix} i\hat{d} - m_0 + \mathcal{M}\gamma^0 - \sigma - i\gamma^5 \vec{\tau} \vec{\pi}, & -i\gamma^5 \sigma_2 \tau_2 \Delta \\ -i\gamma^5 \sigma_2 \tau_2 \Delta^*, & i\hat{d} - m_0 - \gamma^0 \mathcal{M} - \sigma - i\gamma^5 (\vec{\tau})^T \vec{\pi} \end{pmatrix}. \quad (9)$$

Notice that matrix elements of the  $2 \times 2$  matrix  $Z$ , i.e., the quantities  $D^\pm$ ,  $K$ , and  $K^*$ , are the nontrivial operators in the  $(3+1)$ -dimensional coordinate, four-dimensional spinor, 2-dimensional flavor and ( $N_c = 2$ )-dimensional color spaces. Then, in the one fermion-loop (or mean-field

$$\begin{aligned} \sigma(x) &= -2H(\bar{q}q), \\ \Delta(x) &= -2H[\bar{q}^c i\gamma^5 \sigma_2 \tau_2 q] = -2H[q^T C i\gamma^5 \sigma_2 \tau_2 q], \\ \vec{\pi}(x) &= -2H(\bar{q}i\gamma^5 \vec{\tau} q), \\ \Delta^*(x) &= -2H[\bar{q}i\gamma^5 \sigma_2 \tau_2 q^c] = -2H[\bar{q}i\gamma^5 \sigma_2 \tau_2 C \bar{q}^T]. \end{aligned} \quad (6)$$

It is easy to see from Eq. (6) that  $\sigma(x)$  and  $\pi_a(x)$  ( $a = 1, 2, 3$ ) are Hermitian, i.e., real, bosonic fields, whereas  $\Delta^*(x)$  and  $\Delta(x)$  are Hermitian conjugated to each other. Indeed, one can check that  $(\sigma(x))^\dagger = \sigma(x)$ ,  $(\pi_a(x))^\dagger = \pi_a(x)$ ,  $(\Delta(x))^\dagger = \Delta^*(x)$  and  $(\Delta^*(x))^\dagger = \Delta(x)$ , where the superscript symbol  $\dagger$  denotes the Hermitian conjugation. Note that the composite bosonic field  $\pi_3(x)$  can be identified with the physical  $\pi^0(x)$ -meson field, whereas the physical  $\pi^\pm(x)$ -meson fields are the following combinations of the composite fields,  $\pi^\pm(x) = (\pi_1(x) \mp i\pi_2(x))/\sqrt{2}$ . It is clear that the ground state expectation values of all boson fields (6) are  $SU(2)_c$  invariants, hence in this model the color symmetry cannot be broken dynamically. If the ground state expectation values  $\langle \sigma(x) \rangle \neq 0$  or  $\langle \pi_0(x) \rangle \neq 0$ , then chiral symmetry  $U(1)_{A_{I_3}}$  of the model (1) is broken spontaneously. If in the ground state we have  $\langle \pi_{1,2}(x) \rangle \neq 0$ , then isospin  $U(1)_{I_3}$  is broken spontaneously. This phase of quark matter is called the charged pion condensation (PC) phase. Finally, if  $\langle \Delta(x) \rangle \neq 0$ , then in the system spontaneous breaking of the baryon  $U(1)_B$  symmetry occurs, and the baryon superfluid (BSF) phase is realized in the model.

Introducing the Nambu-Gorkov bispinor field  $\Psi$ , where

$$\begin{aligned} \Psi &= \begin{pmatrix} q \\ q^c \end{pmatrix}, & \Psi^T &= (q^T, \bar{q}C^{-1}); \\ \bar{\Psi} &= (\bar{q}, \bar{q}^c) = (\bar{q}, q^T C) = \Psi^T \begin{pmatrix} 0 & C \\ C & 0 \end{pmatrix} \equiv \Psi^T Y, \end{aligned} \quad (7)$$

one can bring the auxiliary Lagrangian (5) to the following form

$$\tilde{L} = -\frac{\sigma^2 + \vec{\pi}^2 + \Delta^* \Delta}{4H} + \frac{1}{2} \Psi^T (YZ) \Psi, \quad (8)$$

where matrix  $Y$  is defined in Eq. (7) and

approximation, the effective action  $\mathcal{S}_{\text{eff}}(\sigma, \vec{\pi}, \Delta, \Delta^*)$  of the model (1)–(5) [this quantity is the generating functional of one-particle irreducible Green functions of boson fields (6)] is expressed by means of the path integral over quark fields:

$$\exp(i\mathcal{S}_{\text{eff}}(\sigma, \vec{\pi}, \Delta, \Delta^*)) = N' \int [d\vec{q}][dq] \exp\left(i \int \tilde{L} d^4x\right), \quad (10)$$

where  $N'$  is a normalization constant and

$$\mathcal{S}_{\text{eff}}(\sigma, \vec{\pi}, \Delta, \Delta^*) = - \int d^4x \left[ \frac{\sigma^2(x) + \vec{\pi}^2(x) + |\Delta(x)|^2}{4H} \right] + \tilde{\mathcal{S}}_{\text{eff}}. \quad (11)$$

The quark contribution to the effective action, i.e., the term  $\tilde{\mathcal{S}}_{\text{eff}}$  in (11), is given by:

$$\exp(i\tilde{\mathcal{S}}_{\text{eff}}) = N' \int [d\vec{q}][dq] \exp\left(\frac{i}{2} \int [\Psi^T(YZ)\Psi] d^4x\right). \quad (12)$$

Note that in Eqs. (10)–(12) we have used the expression (8) for the auxiliary Lagrangian  $\tilde{L}$ . Since the integration measure in Eq. (12) obeys the relation  $[d\vec{q}][dq] = [dq^c][dq] = [d\Psi]$ , we have from it

$$\exp(i\tilde{\mathcal{S}}_{\text{eff}}) = \int [d\Psi] \exp\left\{\frac{i}{2} \int \Psi^T(YZ)\Psi d^4x\right\} = \det^{1/2}(YZ) = \det^{1/2}(Z), \quad (13)$$

where the last equality is valid due to the evident relation  $\det Y = 1$ . Then, using the Eqs. (11) and (13) one can obtain the following expression for the effective action (11):

$$\mathcal{S}_{\text{eff}}(\sigma, \vec{\pi}, \Delta, \Delta^*) = - \int d^4x \left[ \frac{\sigma^2(x) + \vec{\pi}^2(x) + |\Delta(x)|^2}{4H} \right] - \frac{i}{2} \ln \det(Z). \quad (14)$$

Starting from Eq. (14), one can define in the mean-field approximation the thermodynamic potential (TDP)  $\Omega(\sigma, \vec{\pi}, \Delta, \Delta^*)$  of the model (1)–(5),

$$\mathcal{S}_{\text{eff}}|_{\sigma, \vec{\pi}, \Delta, \Delta^* = \text{const}} = -\Omega(\sigma, \vec{\pi}, \Delta, \Delta^*) \int d^4x. \quad (15)$$

The ground state expectation values (mean values) of the fields:  $\langle \sigma(x) \rangle \equiv \sigma$ ,  $\langle \vec{\pi}(x) \rangle \equiv \vec{\pi}$ ,  $\langle \Delta(x) \rangle \equiv \Delta$ ,  $\langle \Delta^*(x) \rangle \equiv \Delta^*$ , are the solutions of the gap equations for the TDP  $\Omega$  (below, in our approach all ground state expectation values  $\sigma$ ,  $\vec{\pi}$ ,  $\Delta$ ,  $\Delta^*$  do not depend on coordinates  $x$ ):

$$\frac{\partial \Omega}{\partial \pi_a} = 0, \quad \frac{\partial \Omega}{\partial \sigma} = 0, \quad \frac{\partial \Omega}{\partial \Delta} = 0, \quad \frac{\partial \Omega}{\partial \Delta^*} = 0. \quad (16)$$

Since the matrix  $Z$  in Eq. (14) has an evident  $2 \times 2$  block structure [see in Eq. (9)], one can use there a general formula

$$\det \begin{pmatrix} A & B \\ C & D \end{pmatrix} = \det[-CB + CAC^{-1}D] = \det[DA - DBD^{-1}C], \quad (17)$$

and find that (taking into account the relation  $\tau_2 \vec{\tau} \tau_2 = -\vec{\tau}^T$  and assuming that all bosonic fields do not depend on  $x$ )

$$\begin{aligned} \det(Z) &\equiv \det \begin{pmatrix} D^+ & K \\ K^* & D^- \end{pmatrix} \\ &= \det(-K^*K + K^*D^+K^{*-1}D^-) \\ &= \det[\Delta^* \Delta + (-i\hat{\partial} - m_0 - \widetilde{\mathcal{M}}\gamma^0 - \sigma + i\gamma^5(\vec{\tau})^T \vec{\pi}) \\ &\quad \times (i\hat{\partial} - m_0 - \gamma^0 \mathcal{M} - \sigma - i\gamma^5(\vec{\tau})^T \vec{\pi})], \end{aligned} \quad (18)$$

where

$$\widetilde{\mathcal{M}} = \mu + \mu_5 \gamma^5 - \nu \tau_3 - \nu_5 \gamma^5 \tau_3. \quad (19)$$

Obviously, the quantity which is in the square brackets of Eq. (18) is proportional to the unit operator in the  $N_c$ -color space. (Below, in all numerical calculations we put  $N_c = 2$ .) Hence,

$$\det(Z) = \det^{N_c} \mathcal{D} \equiv \det^{N_c} \begin{pmatrix} D_{11} & D_{12} \\ D_{21} & D_{22} \end{pmatrix}, \quad (20)$$

where  $\mathcal{D}$  is the  $2 \times 2$  matrix in the 2-dimensional flavor space (its matrix elements  $D_{kl}$  are the nontrivial operators in the 4-dimensional spinor and in the  $(3+1)$ -dimensional coordinate spaces). Using this expression for  $\det(Z)$  in Eq. (14) when  $\sigma$ ,  $\vec{\pi}$ ,  $\Delta$ ,  $\Delta^*$  do not depend on coordinates  $x$ , and taking into account the well-known technique for calculating determinants of operators (see, for example, Eq. (A6) of Appendix A from Ref. [41]), we find

$$\begin{aligned} \mathcal{S}_{\text{eff}}(\sigma, \pi_a, \Delta, \Delta^*)|_{\sigma, \vec{\pi}, \Delta, \Delta^* = \text{const}} &= - \frac{\sigma^2 + \vec{\pi}^2 + |\Delta|^2}{4H} \int d^4x - \frac{iN_c}{2} \ln \det \mathcal{D} \\ &= - \frac{\sigma^2 + \vec{\pi}^2 + |\Delta|^2}{4H} \int d^4x \\ &\quad - \frac{iN_c}{2} \int \frac{d^4p}{(2\pi)^4} \ln \det \overline{\mathcal{D}}(p) \int d^4x, \end{aligned} \quad (21)$$

where the  $2 \times 2$  matrix  $\overline{\mathcal{D}}(p)$  is the momentum space representation of the matrix  $\mathcal{D}$  of Eq. (20). Its matrix elements  $\overline{\mathcal{D}}_{kl}(p)$  have the following form

$$\begin{aligned}
\overline{D}_{11}(p) &= |\Delta|^2 - p^2 + (\mu + \mu_5\gamma^5)[\hat{p}\gamma^0 - \gamma^0\hat{p}] \\
&\quad + (\nu + \nu_5\gamma^5)[\hat{p}\gamma^0 + \gamma^0\hat{p}] + \vec{\pi}^2 + M^2 \\
&\quad + 2M\gamma^0(\mu + \nu_5\gamma^5) + (\mu + \mu_5\gamma^5)^2 - (\nu + \nu_5\gamma^5)^2 \\
&\quad + 2i\mu\gamma^0\gamma^5\pi_3 + 2i\nu_5\gamma^0\pi_3, \\
\overline{D}_{22}(p) &= |\Delta|^2 - p^2 + (\mu + \mu_5\gamma^5)[\hat{p}\gamma^0 - \gamma^0\hat{p}] \\
&\quad - (\nu + \nu_5\gamma^5)[\hat{p}\gamma^0 + \gamma^0\hat{p}] + \vec{\pi}^2 + M^2 \\
&\quad + 2M\gamma^0(\mu - \nu_5\gamma^5) + (\mu + \mu_5\gamma^5)^2 - (\nu + \nu_5\gamma^5)^2 \\
&\quad - 2i\mu\gamma^0\gamma^5\pi_3 + 2i\nu_5\gamma^0\pi_3, \\
\overline{D}_{12}(p) &= 2i\mu\gamma^0\gamma^5(\pi_1 + i\pi_2) + 2\nu\gamma^0\gamma^5(\pi_2 - i\pi_1) \\
&= 2\gamma^0\gamma^5(\nu - \mu)[\pi_2 - i\pi_1], \\
\overline{D}_{21}(p) &= 2i\mu\gamma^0\gamma^5(\pi_1 - i\pi_2) + 2\nu\gamma^0\gamma^5(i\pi_1 + \pi_2) \\
&= 2\gamma^0\gamma^5(\nu + \mu)[\pi_2 + i\pi_1], \tag{22}
\end{aligned}$$

where  $M \equiv m_0 + \sigma$ ,  $p^2 = p^\rho p_\rho$ ,  $\hat{p} = \gamma^\rho p_\rho$ . Using in Eq. (21) again the general relation (17), we have

$$\begin{aligned}
\det \overline{D}(p) &\equiv \det \begin{pmatrix} \overline{D}_{11}(p), & \overline{D}_{12}(p) \\ \overline{D}_{21}(p), & \overline{D}_{22}(p) \end{pmatrix} \\
&= \det[-\overline{D}_{21}(p)\overline{D}_{12}(p) \\
&\quad + \overline{D}_{21}(p)\overline{D}_{11}(p)(\overline{D}_{21}(p))^{-1}\overline{D}_{22}(p)] \\
&\equiv \det L(p). \tag{23}
\end{aligned}$$

Notice that the matrix  $L(p)$ , i.e., the expression in square brackets of Eq. (23), is indeed a  $4 \times 4$  matrix in 4-dimensional spinor space only, which is composed of  $4 \times 4$  matrices  $\overline{D}_{ij}(p)$  [see in Eq. (22)]. Now, taking into account the definition (15) and using the Eqs. (21)–(23), it is possible to obtain in the mean-field approximation the TDP of the model,

$$\begin{aligned}
\Omega(M, \vec{\pi}, \Delta, \Delta^*) &= \frac{(M - m_0)^2 + \vec{\pi}^2 + |\Delta|^2}{4H} \\
&\quad + \frac{iN_c}{2} \int \frac{d^4 p}{(2\pi)^4} \ln \det L(p). \tag{24}
\end{aligned}$$

Since  $\det L(p) = \lambda_1(p)\lambda_2(p)\lambda_3(p)\lambda_4(p)$ , where  $\lambda_i(p)$  ( $i = 1, \dots, 4$ ) are four eigenvalues of the  $4 \times 4$  matrix  $L(p)$ , in the following, in order to find the TDP of the model in various cases, we will first of all find the eigenvalues of the matrix  $L(p)$ . Then, after integration in Eq. (24) over  $p_0$ , this TDP is used in some numerical calculations with sharp three-momentum cutoff  $\Lambda = 657$  MeV (i.e., it is assumed below that the integration over three-momentum  $\vec{p}$  occurs over the region  $|\vec{p}| < \Lambda$ ) at  $H = 7.23$  GeV<sup>-2</sup> and  $m_0 = 5.4$  MeV [14,15]. Moreover, we study also the phase

structure of the model in the chiral limit,  $m_0 = 0$ , at the same values of  $\Lambda$  and  $H$ .

Note that at first glance, the TDP (24) looks like a function of six variables (condensates),  $M$ ,  $\vec{\pi}$ ,  $\Delta$ , and  $\Delta^*$ . But due to a symmetry of the model, the number of condensates that characterize the ground state of a system may be reduced. Indeed, at  $m_0 = 0$  and zero chemical potentials the Lagrangian (1) is invariant under  $SU(4) \times U(1)_B \times SU(2)_c$  group. As a consequence of this symmetry, the TDP is a function of only one single variable ( $M^2 + |\Delta|^2 + \vec{\pi}^2$ ). And this fact significantly simplifies the analysis of the function (24) on the global minimum. If nonzero chemical potentials are taken into consideration, then in the chiral limit the symmetry of the Lagrangian (1) reduces to  $U(1)_B \times U(1)_{I_3} \times U(1)_{AI_3}$  (plus color  $SU(2)_c$ , which in our consideration is not violated at all). As a result, we see that at  $m_0 = 0$  and nonzero chemical potentials the TDP of the model depends only on the  $|\Delta|^2$ ,  $\pi_1^2 + \pi_2^2$  and  $M^2 + \pi_0^2$  field combinations, correspondingly. So without loss of generality of consideration, in the chiral limit we can put  $\pi_0 = 0$  and  $\pi_2 = 0$ . However, at  $m_0 \neq 0$  and at nonzero chemical potentials the symmetry of the model Lagrangian reduces to  $U_B(1) \times U_{I_3}(1)$ , i.e., in this case the TDP depends on  $|\Delta|$ ,  $M$ ,  $\pi_0$  and  $\pi_1^2 + \pi_2^2$ . So in this case without loss of generality we can also put  $\pi_2 = 0$ . Moreover, at  $m_0 \neq 0$ , as it was argued in our previous paper [41], it is possible to put  $\pi_0 = 0$  as well. Hence, below throughout the paper we suppose that the TDP (24) is a function of only  $M$ ,  $\pi_1$  and  $|\Delta|$  condensates. Others are zero.

### III. CALCULATION OF THE TDP (24) AND ITS DUALITY PROPERTIES

#### A. The case of $\mu \neq 0$ , $\nu \neq 0$ , $\nu_5 \neq 0$ , but $\mu_5 = 0$

First, let us suppose that chiral chemical potential  $\mu_5$  is equal to zero. The rest of chemical potentials, i.e.,  $\mu$ ,  $\nu$  and  $\nu_5$ , we will call the basic chemical potentials, since (i) they correspond to the conserved charges of the model, and (ii) it is they that largely determine the phase structure of the model. In this case when  $\mu \neq 0$ ,  $\nu \neq 0$ , and  $\nu_5 \neq 0$  the matrix  $L(p)$  of Eqs. (23) and (24) has four different eigenvalues  $\lambda_i(p)$  (they can be found with the help of any program of analytical calculations),

$$\lambda_{1,2}(p) = N_1 \pm 4\sqrt{K_1}, \quad \lambda_{3,4}(p) = N_2 \pm 4\sqrt{K_2}, \tag{25}$$

where

$$\begin{aligned}
N_2 &= N_1 + 16\mu\nu\nu_5|\vec{p}|, \\
K_2 &= K_1 + 8\mu\nu\nu_5|\vec{p}|p_0^4 - 8\mu\nu\nu_5|\vec{p}|p_0^2(M^2 + \pi_1^2 + |\Delta|^2 \\
&\quad + |\vec{p}|^2 + \mu^2 + \nu^2 - \nu_5^2), \tag{26}
\end{aligned}$$

$$K_1 = \nu_3^2 p_0^6 - p_0^4 [2\nu_5^2 (|\Delta|^2 + \pi_1^2 + M^2 + |\vec{p}|^2 + \nu^2 + \mu^2 - \nu_5^2) + 4\mu\nu\nu_5 |\vec{p}|] + p_0^2 \{\nu_5^6 + 2\nu_5^4 (M^2 - |\Delta|^2 - \pi_1^2 - \nu^2 - \mu^2 - |\vec{p}|^2) + 4\mu^2 \nu^2 (M^2 + |\vec{p}|^2) + 4|\vec{p}| \mu \nu \nu_5 (|\Delta|^2 + \pi_1^2 + M^2 + |\vec{p}|^2 + \nu^2 + \mu^2 - \nu_5^2) + \nu_5^2 [ (|\Delta|^2 + \pi_1^2 + |\vec{p}|^2 + \nu^2 + \mu^2)^2 + 2|\vec{p}|^2 M^2 + M^4 + 2M^2 (|\Delta|^2 - \nu^2 + \pi_1^2 - \mu^2)] \}, \quad (27)$$

$$N_1 = p_0^4 - 2p_0^2 [|\Delta|^2 + \pi_1^2 + M^2 + |\vec{p}|^2 + \nu^2 + \mu^2 - 3\nu_5^2] + \nu_5^4 - 2\nu_5^2 [|\Delta|^2 + \pi_1^2 + |\vec{p}|^2 + \nu^2 + \mu^2 - M^2] - 8\mu\nu\nu_5 |\vec{p}| + (|\vec{p}|^2 + M^2 + \pi_1^2 + |\Delta|^2 - \mu^2 - \nu^2)^2 - 4(\mu^2 \nu^2 - \pi_1^2 \nu^2 - |\Delta|^2 \mu^2), \quad (28)$$

and the TDP (24) has the form

$$\Omega(M, \pi_1, |\Delta|) = \frac{(M - m_0)^2 + \pi_1^2 + |\Delta|^2}{4H} + \frac{iN_c}{2} \int \frac{d^4 p}{(2\pi)^4} \{ \ln(\lambda_1(p)\lambda_2(p)) + \ln(\lambda_3(p)\lambda_4(p)) \}. \quad (29)$$

It is possible to show that the TDP (29) is an even with respect to each of the three transformations,  $\mu \rightarrow -\mu$ ,  $\nu \rightarrow -\nu$  and  $\nu_5 \rightarrow -\nu_5$ . Indeed, if, e.g.,  $\mu \rightarrow -\mu$  then, as it follows from Eqs. (25)–(28), we have  $\lambda_1(p) \leftrightarrow \lambda_3(p)$  and  $\lambda_2(p) \leftrightarrow \lambda_4(p)$ . Hence, when the sign of the chemical potential  $\mu$  changes, the TDP (29) itself remains invariant, etc. It means that without loss of generality we can use only the positive values of the basic chemical potentials. More interesting is the fact that each of the eigenvalues  $\lambda_i(p)$  (25) is invariant with respect to the so-called dual transformation  $\mathcal{D}_1$ ,

$$\mathcal{D}_1: \mu \leftrightarrow \nu, \quad \pi_1 \leftrightarrow |\Delta|. \quad (30)$$

As a result, at  $\mu_5 = 0$ , and even at  $m_0 \neq 0$ , the whole TDP (24) or (29) of the model is also invariant under the transformation (30). Moreover, using any program of analytical calculations, it is possible to establish that each of the products  $\lambda_1(p)\lambda_2(p)$  and  $\lambda_3(p)\lambda_4(p)$  is invariant in addition with respect to the following two dual discrete transformations  $\mathcal{D}_2$  and  $\mathcal{D}_3$ , where

$$\begin{aligned} \mathcal{D}_2: \mu &\leftrightarrow \nu_5, & M &\leftrightarrow |\Delta|; \\ \mathcal{D}_3: \nu &\leftrightarrow \nu_5, & M &\leftrightarrow \pi_1. \end{aligned} \quad (31)$$

This fact was proved in Ref. [41]. As a result, we see that at  $m_0 = 0$  the TDP (29) is invariant under the dual transformations  $\mathcal{D}_2$  and  $\mathcal{D}_3$  (31) in addition to  $\mathcal{D}_1$  (30). (Note that at  $m_0 \neq 0$  it is invariant only under the  $\mathcal{D}_1$  (30) transformation.)

## B. The case of all nonzero chemical potentials

Now, let us consider the case when  $\mu_5 \neq 0$  is taken into account in addition to the basic chemical potentials  $\mu \neq 0$ ,  $\nu \neq 0$  and  $\nu_5 \neq 0$ . It is possible to show that in this case the

matrix  $L(p)$  of Eqs. (23) and (24) has four different eigenvalues  $\tilde{\lambda}_i(p)$ ,

$$\begin{aligned} \tilde{\lambda}_{1,2}(p) &= \lambda_{1,2}(p)|_{|\vec{p}| \rightarrow |\vec{p}| - \mu_5}, \\ \tilde{\lambda}_{3,4}(p) &= \lambda_{3,4}(p)|_{|\vec{p}| \rightarrow |\vec{p}| + \mu_5}, \end{aligned} \quad (32)$$

where  $\lambda_i(p)$  are the eigenvalues (25) of the  $L(p)$  at  $\mu_5 = 0$ . Hence in the most general case we obtain the following expression for the TDP (24)

$$\Omega(M, \pi_1, |\Delta|) = \frac{(M - m_0)^2 + \pi_1^2 + |\Delta|^2}{4H} + \frac{iN_c}{2} \int \frac{d^4 p}{(2\pi)^4} \{ \ln(\tilde{\lambda}_1(p)\tilde{\lambda}_2(p)) + \ln(\tilde{\lambda}_3(p)\tilde{\lambda}_4(p)) \}. \quad (33)$$

Due to the relations (32), it is clear that the chemical potential  $\mu_5$  does not spoil the dual symmetries inherent to the TDP (29) in the case  $\mu_5 = 0$ . So, at  $m_0 \neq 0$  the TDP (24) or (33) is invariant with respect to the dual  $\mathcal{D}_1$  (30) transformation, whereas in the chiral limit,  $m_0 = 0$ , it is invariant with respect to the  $\mathcal{D}_2$  and  $\mathcal{D}_3$  (31) duality transformations, in addition. It is one of the main results of the paper.

It is clear directly from the relations (32) that if one of the chemical potentials is equal to zero, then  $\Omega(M, \pi_1, |\Delta|)$  is an even function with respect to each of the rest nonzero chemical potentials. However, if all four chemical potentials  $\mu$ ,  $\nu$ ,  $\nu_5$ , and  $\mu_5$  are nonzero, then it is easily seen from relations (32) and (25)–(28) that the TDP (33) is invariant with respect to each of the following six transformations, in each of them two chemical potentials change their sign simultaneously: (i)  $\{\nu \rightarrow -\nu; \nu_5 \rightarrow -\nu_5\}$ , (ii)  $\{\nu \rightarrow -\nu; \mu_5 \rightarrow -\mu_5\}$ , (iii)  $\{\nu_5 \rightarrow -\nu_5; \mu_5 \rightarrow -\mu_5\}$ , (iv)  $\{\mu \rightarrow -\mu; \mu_5 \rightarrow -\mu_5\}$ , (v)  $\{\mu \rightarrow -\mu; \nu \rightarrow -\nu\}$ , and (vi)  $\{\mu \rightarrow -\mu; \nu_5 \rightarrow -\nu_5\}$ . The invariance of the TDP (33) under the transformations (i)–(vi) can help to simplify the analysis of the phase portrait of the model. In particular, it is sufficient to study the phase structure of the model only, e.g., in the case when arbitrary three of the four chemical potentials have positive signs, whereas the sign of the rest chemical potential is not fixed. Then, applying to a phase diagram



with this particular distribution of the chemical potential signs one or several transformations (i)–(vi), it is possible to find a phase portrait of the model at an arbitrary distribution of chemical potential signs. Hence, in the following we will study the phase diagram of the model only at  $\mu \geq 0$ ,  $\nu \geq 0$ ,  $\nu_5 \geq 0$  and for arbitrary sign of  $\mu_5$ .

Note that in our previous article [41], where the chiral asymmetry of the two-color dense quark system was investigated in the form of only  $\mu_{15} \neq 0$  but  $\mu_5 = 0$ , it was argued that in the chiral limit,  $m_0 = 0$ , for sufficiently low values of the chemical potentials (say at  $\mu, \nu, \nu_5 < 1$  GeV) at the global minimum point (GMP)  $(M, \pi_1, |\Delta|)$  of the TDP (29), there can be no more than one nonzero coordinates, i.e., condensates or order parameters. (The particular argument could be that in previous investigations there have not been found (mixed) phases with several nonzero condensates, e.g., in the three-color NJL model [29] and in the two-color one [6,15].) Therefore, with such a restriction on chemical potentials, in the chiral limit only four different phases can be realized in the system. (I) If

GMP has the form  $(M \neq 0, \pi_1 = 0, |\Delta| = 0)$ , then the chiral symmetry breaking (CSB) phase appears in the model. (II) If it has the form  $(M = 0, \pi_1 \neq 0, |\Delta| = 0)$ , the charged pion condensation (PC) phase is realized. (III) When the GMP looks like  $(M = 0, \pi_1 = 0, |\Delta| \neq 0)$ , it corresponds to the baryon superfluid (BSF) or diquark condensation phase. And finally, (IV) the GMP of the form  $(M = 0, \pi_1 = 0, |\Delta| = 0)$  corresponds to a symmetrical phase with all zero condensates.

In a similar way, in the present paper we suppose that if, in addition, the chemical potential  $\mu_5$  is taken into account, then the GMP of the TDP (33) has the same structure, and only four above mentioned phases (I)–(IV) are allowed to exist in the system. Thanks to this structure of the global minimum point, we see that in the region of relatively low values of the chemical potentials it is enough to study not the whole TDP (33), but only its projections on the condensate axis,  $F_1(M) \equiv \Omega(M, \pi_1 = 0, |\Delta| = 0)$ ,  $F_2(\pi_1) \equiv \Omega(M = 0, \pi_1, |\Delta| = 0)$  and  $F_3(|\Delta|) \equiv \Omega(M = 0, \pi_1 = 0, |\Delta|)$ , where

$$F_1(M) = \frac{M^2}{4H} - \frac{N_c}{2} \sum_{\pm} \int \frac{d^3p}{(2\pi)^3} \left[ \left| \mu + \nu \pm \sqrt{M^2 + (|\vec{p}| - \mu_5 - \nu_5)^2} \right| + \left| \mu - \nu \pm \sqrt{M^2 + (|\vec{p}| - \mu_5 + \nu_5)^2} \right| \right. \\ \left. + \left| \mu + \nu \pm \sqrt{M^2 + (|\vec{p}| + \mu_5 + \nu_5)^2} \right| + \left| \mu - \nu \pm \sqrt{M^2 + (|\vec{p}| + \mu_5 - \nu_5)^2} \right| \right], \quad (34)$$

$$F_2(\pi_1) = \frac{\pi_1^2}{4H} - \frac{N_c}{2} \sum_{\pm} \int \frac{d^3p}{(2\pi)^3} \left[ \left| \mu + \nu_5 \pm \sqrt{\pi_1^2 + (|\vec{p}| - \mu_5 - \nu)^2} \right| + \left| \mu - \nu_5 \pm \sqrt{\pi_1^2 + (|\vec{p}| - \mu_5 + \nu)^2} \right| \right. \\ \left. + \left| \mu + \nu_5 \pm \sqrt{\pi_1^2 + (|\vec{p}| + \mu_5 + \nu)^2} \right| + \left| \mu - \nu_5 \pm \sqrt{\pi_1^2 + (|\vec{p}| + \mu_5 - \nu)^2} \right| \right], \quad (35)$$

$$F_3(|\Delta|) = \frac{|\Delta|^2}{4H} - \frac{N_c}{2} \sum_{\pm} \int \frac{d^3p}{(2\pi)^3} \left[ \left| \nu_5 + \nu \pm \sqrt{|\Delta|^2 + (|\vec{p}| - \mu_5 - \mu)^2} \right| + \left| \nu_5 - \nu \pm \sqrt{|\Delta|^2 + (|\vec{p}| - \mu_5 + \mu)^2} \right| \right. \\ \left. + \left| \nu_5 + \nu \pm \sqrt{|\Delta|^2 + (|\vec{p}| + \mu_5 + \mu)^2} \right| + \left| \nu_5 - \nu \pm \sqrt{|\Delta|^2 + (|\vec{p}| + \mu_5 - \mu)^2} \right| \right]. \quad (36)$$

(At  $\mu_5 = 0$  these projections have been obtained in Appendix C of Ref. [41]. The contribution of the  $\mu_5 \neq 0$  can be taken into account by the procedure (32). Throughout the paper the integration over the three-momentum  $\vec{p}$  in Eqs. (34)–(36) occurs in the region  $|\vec{p}| < \Lambda = 657$  MeV.) Then, comparing the smallest values of these functions, we can determine the GMP of the initial TDP (33), and, therefore, the phase in which the system is located in the chiral limit,  $m_0 = 0$ , at given values of chemical potentials. The behavior of the GMP of the model thermodynamic potential (33) vs chemical potentials supplies us with the full  $(\mu, \nu, \nu_5, \mu_5)$ -phase portrait of the two-color NJL model (1). Indeed, it is no more than a one-to-one correspondence between any point  $(\mu, \nu, \nu_5, \mu_5)$  of the four-dimensional space of chemical

potentials and possible model phases (CSB, charged PC, BSF, and symmetric phase). However, it is clear that this four-dimensional phase portrait (diagram) is quite bulky and it is rather hard to imagine it as a whole. So in order to obtain a more deep understanding of the phase diagram as well as to get a greater visibility of it, it is very convenient to consider different low-dimensional cross sections of this general  $(\mu, \mu_5, \nu, \nu_5)$ -phase portrait, defined by the constraints of the form  $\nu = \text{const}$  or  $\mu_5 = \text{const}$  and  $\nu_5 = \text{const}$ , etc. In the next Sec. IV these different cross sections of the most general phase portrait will be presented. But before that, let us discuss the role and influence of the dual symmetries  $\mathcal{D}_1$  (30),  $\mathcal{D}_2$  and  $\mathcal{D}_3$  (31) of the model TDP on the shape of its different phase portraits (see also the relevant paper [41]).

### C. Dual symmetries of the TDP (33) and phase portraits of the model at $\mu_5 \neq 0$

As it is clear from the previous subsections, chiral chemical potential  $\mu_5 \neq 0$  does not spoil symmetries of the model TDP with respect to duality transformations (30) and (31), observed first of all at  $\mu_5 = 0$ .

Recall that by duality property (or symmetry, or relation, etc) of any model, we understand any discrete symmetry of its TDP with respect to transformations as order parameters (in our case, condensates  $M$ ,  $\pi_1$  and  $|\Delta|$ ) and free external parameters of the system (these may be chemical potentials, coupling constants, etc.) The presence of the dual symmetry of the model TDP means that in its phase portrait there is some symmetry between phases with respect to the transformation of external parameters, which can greatly simplify the construction of the full phase diagram of the system. (The invariance of the TDP (33) with respect to sign reversal for any two of the four chemical potentials is the simplest example of the dual symmetry of the model (1). Due to this kind of duality, it is enough to study the phase structure of the model only, e.g., at  $\mu \geq 0$ ,  $\nu \geq 0$ ,  $\nu_5 \geq 0$  and for arbitrary sign of  $\mu_5$ , etc.) Below, we investigate the phase portrait of the model (1) in the mean-field approximation in the presence of four nonzero chemical potentials,  $\mu$ ,  $\nu$ ,  $\nu_5$ , and  $\mu_5$  in the chiral limit, putting a special attention to the role of  $\mu_5$  in its formation. In this case, the problem is greatly simplified due to the fact that the model TDP (33) has three dual symmetries,  $\mathcal{D}_1$  (30) and  $\mathcal{D}_2$ ,  $\mathcal{D}_3$  (31).

Indeed, let us suppose that  $m_0 = 0$  and that at the point  $(\mu = a, \nu = b, \nu_5 = c, \mu_5 = d)$  of the phase portrait the GMP of the TDP (33) lies, e.g., at the point of the condensate space of the form  $(M = A, \pi_1 = 0, |\Delta| = 0)$ , i.e., in this case the CSB phase is realized in the system. Then, according to the symmetries  $\mathcal{D}_2$  and  $\mathcal{D}_3$  (31), the TDP has the same meaning if we interchange the values of chemical potentials and simultaneously appropriately transpose the values of the condensates. As a result we see that, e.g., at  $\mu = c, \nu = b, \nu_5 = a, \mu_5 = d$  and in the point  $(M = 0, \pi_1 = 0, |\Delta| = A)$  (it is the result of the action of the  $\mathcal{D}_2$  dual transformation on the TDP (33)) as well as that at  $\mu = a, \nu = c, \nu_5 = b, \mu_5 = d$  and in the point  $(M = 0, \pi_1 = A, |\Delta| = 0)$  (it is the application of the  $\mathcal{D}_3$  dual transformation to the TDP) it has the initial meaning. Moreover, it is evident that these new points of the condensate space are nothing but the GMPs of the TDP (33) after its  $\mathcal{D}_2$  and  $\mathcal{D}_3$  transformations (see a more detailed discussion in Ref. [41]). Consequently, at the points  $(\mu = c, \nu = b, \nu_5 = a, \mu_5 = d)$  and  $(\mu = a, \nu = c, \nu_5 = b, \mu_5 = d)$  of the phase diagram of the model, which we call dually  $\mathcal{D}_2$  and dually  $\mathcal{D}_3$  conjugated to the starting point  $(\mu = a, \nu = b, \nu_5 = c, \mu_5 = d)$  of the phase portrait, there are BSF and charged PC phases that are respectively dually  $\mathcal{D}_2$  and dually  $\mathcal{D}_3$  conjugated to the initial CSB phase of the model. Thus, knowing the phase of the model, which is realized at some point of its phase portrait, we can predict

which phases are arranged at the dually conjugated points of a phase diagram. Moreover, the order parameter of the initial CSB phase of the point  $(\mu = a, \nu = b, \nu_5 = c, \mu_5 = d)$ , i.e., the quantity  $M = A$ , is equal to the order parameter  $|\Delta| = A$  of the  $\mathcal{D}_2$ -dually conjugated BSF phase of the point  $(\mu = c, \nu = b, \nu_5 = a, \mu_5 = d)$  of the model phase portrait, etc.

At  $m_0 = 0$  each duality transformation  $\mathcal{D}_i$  ( $i = 1, 2, 3$ ) (30) and (31) of the TDP can also be applied to an arbitrary phase portrait of the model as a whole. In particular, it is clear that if we have a most general  $(\mu, \nu, \nu_5, \mu_5)$ -phase portrait, then the action, e.g., of the  $\mathcal{D}_3$  on the TDP can be understood as the following dual  $\mathcal{D}_3$  transformation of the model  $(\mu, \nu, \nu_5, \mu_5)$ -phase portrait. Namely, it is necessary to rename both the diagram axes and phases in such a way, that  $\nu \leftrightarrow \nu_5$  and CSB  $\leftrightarrow$  charged PC. At the same time the  $\mu$ - and  $\mu_5$ -axes and BSF and symmetrical phases should not change their names. It is evident that after such  $\mathcal{D}_3$  transformation the full  $(\mu, \nu, \nu_5, \mu_5)$ -phase diagram is mapped to itself, i.e., the most general  $(\mu, \nu, \nu_5, \mu_5)$ -phase portrait of the model is self- $\mathcal{D}_3$ -dual. In a similar way it is possible to describe the action of other,  $\mathcal{D}_1$  and  $\mathcal{D}_2$ , duality transformations on the full  $(\mu, \nu, \nu_5, \mu_5)$ -phase portrait of the model, which is, of course, invariant, or self-dual, under these mappings. But different cross sections of the full  $(\mu, \nu, \nu_5, \mu_5)$ -phase diagram, e.g., the  $(\mu, \nu)$ -phase portrait at some fixed values of  $\nu_5$  and  $\mu_5$ , are not invariant, in general, under the action of dual transformations (see below for some examples). Finally, note that under any  $\mathcal{D}_i$  ( $i = 1, 2, 3$ ) transformation the symmetrical phase remains intact, i.e., it does not change its position on the phase diagram.

As a result, based on this mechanism of dual transformations of different cross sections of the full phase diagram of the two-color NJL model (1), it is possible, having a well-known phase diagram of the model, to obtain its phase portrait in a less studied range of values of chemical potentials (see some examples from the Ref. [41], as well as the following subsections of this paper). In particular, using this approach, one can draw quite definite conclusions about the effect of chiral asymmetry, i.e.,  $\mu_5$ , on the phase structure of the model (see below).

## IV. PHASE DIAGRAM OF THE MODEL

### A. Phase structure with $\mu_5 \neq 0$ and either one of $\mu, \nu$ and $\nu_5$ is nonzero

Let us start the investigation of the phase structure of the model from a particular and rather simple case when besides nonzero chiral imbalance  $\mu_5$  in quark matter in addition either one of the basic chemical potentials, baryon  $\mu_B \equiv 2\mu$ , isospin  $\mu_I \equiv 2\nu$  or chiral isospin  $\mu_{I5} \equiv 2\nu_5$  chemical potentials, is also nonzero.

First, suppose that only  $\mu_5$  and  $\nu_5$  chemical potentials are nonzero (hence  $\mu = \nu = 0$ ). Then, in the limiting case when  $\mu_5 = 0$  and  $\nu_5 = 0$ , chiral symmetry of the model (1) is

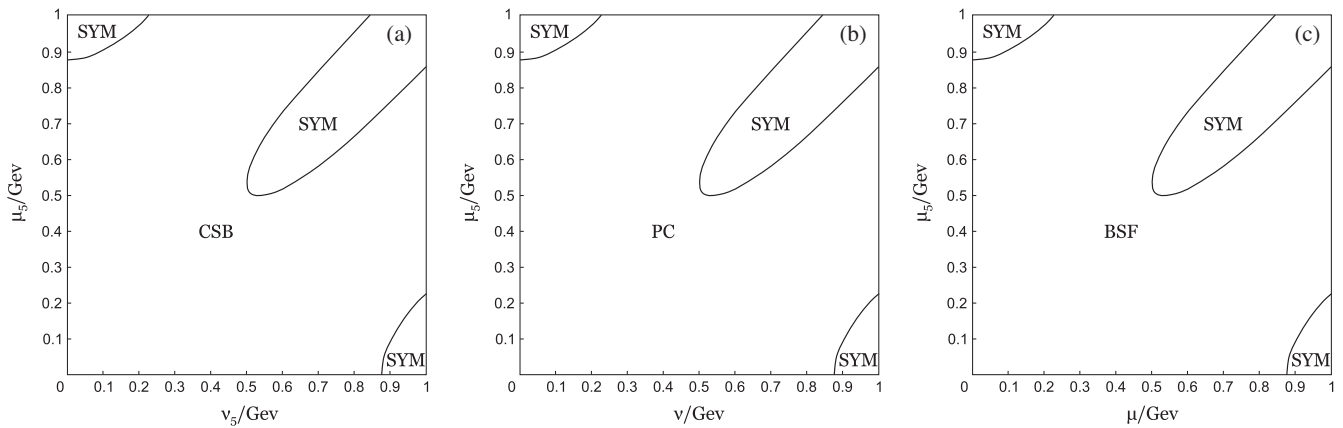


FIG. 1. (a)  $(\nu_5, \mu_5)$ -phase diagram at  $\nu = \mu = 0$  GeV. (b)  $(\nu, \mu_5)$ -phase diagram at  $\mu = \nu_5 = 0$  GeV. (c)  $(\mu, \mu_5)$ -phase diagram at  $\nu_5 = \nu = 0$  GeV. In these diagrams BSF means the baryon superfluid phase, PC—the charged pion condensation phase, CSB—the chiral symmetry breaking, and SYM denotes the symmetrical phase of the model.

broken spontaneously and there is a dynamical generation of nonzero quark mass  $M$  in the system.

The quark matter with chiral  $\mu_5$  imbalance has been considered in Refs. [42,43,45,46]. And it was revealed that if one increases chiral imbalance  $\mu_5$ , then the chiral symmetry breaking phenomenon would consolidate, i.e., the CSB phenomenon would be enhanced and dynamical quark mass  $M$  would increase.<sup>6</sup> This is the so-called effect of catalysis, or enhancement, of chiral symmetry breaking by chiral imbalance that was observed also in three color QCD, but valid and strictly speaking established for the first time on lattice just in two color QCD (see in Ref. [46]). Moreover, in Ref. [41] it was established that in another limiting case,  $\mu_5 = 0$  and  $\nu_5 > 0$ , the CSB phase is also realized at any value of  $\nu_5$  (provided that it is inside the scope of the validity of the model,  $\nu_5 < \Lambda$ ) and catalysis effect was also observed. Starting from the TDP (33) [or comparing the least values of the projections  $F_i$  (34)–(36)], it is possible to obtain the  $(\nu_5, \mu_5)$ -phase portrait of the model at  $\mu = \nu = 0$  [see in Fig. 1(a)].<sup>7</sup> As it is clear from the figure, in this case just the CSB phase occupies all the physically accepted region of chemical potentials,  $\mu_5, \nu_5 < \Lambda$ . Moreover, if one increases any type of chiral imbalances, i.e.,  $\mu_5$  or  $\nu_5$ , then the CSB phenomenon would be enhanced and dynamical quark mass  $M$  value would increase. This could be called the effect of catalysis of

chiral symmetry breaking by chiral imbalance of any form, either  $\mu_5$  or  $\nu_5$ .

In order to support this statement, in Fig. 2(a) the behavior of  $M$  as a function of  $\mu_5$  at, e.g.,  $\nu_5 = 0.1$  GeV is shown for the two-color NJL model (1) at  $\mu = \nu = 0$ . Since this function is an increasing one, we can conclude that CSB is enhanced (or catalysed) by  $\mu_5$  in this case. The behavior of  $M$  vs  $\mu_5$  at other fixed values of  $\nu_5$  is similar. Moreover, in this case, i.e., at  $\mu = \nu = 0$ , the order parameter  $M$  vs  $\nu_5$  at different fixed  $\mu_5$  values is also an increasing function, and in particular at  $\mu_5 = 0.1$  GeV the plot of this function coincides with a curve drawn in Fig. 2(a) in which one should rename  $\mu_5$  axis by  $\nu_5$ . (It follows from the fact that at  $\mu = \nu = 0$  the projection  $F_1(M)$  (34) is symmetrical under the replacement  $\mu_5 \leftrightarrow \nu_5$ .) So increasing at  $\mu = \nu = 0$  either one of chiral imbalances, i.e., chemical potentials  $\mu_5$  or  $\nu_5$ , or both of them simultaneously, the CSB phase only solidifies. In this case the  $(\nu_5, \mu_5)$ -phase structure is not complicated, it is CSB phase everywhere for all physically accepted values of  $\mu_5, \nu_5$ .

This effect could be explained with the following qualitative arguments. The Fermi energies (3) of  $u_L$  and  $u_R$  quarks in this case have a rather simple form  $\mu_{u_L} = \nu_5 + \mu_5$  and  $\mu_{u_R} = -\nu_5 - \mu_5$ . If  $\nu_5 = 0$  then  $\mu_{u_L} = \mu_5$ ,  $\mu_{u_R} = -\mu_5$  and condensation of  $\bar{u}_R u_L$  is quite feasible and this leads to chiral symmetry breaking. One could note also that if  $\mu_5$  is increased, the number of states at Fermi spheres are getting larger and the value of the condensate is increased. The same effect could be observed in the  $\mu_5 = 0$  case and the effect is fully identical,  $\mu_{u_L} = \nu_5$  and  $\mu_{u_R} = -\nu_5$ . The effect of CSB catalysis simultaneously by both  $\mu_5$  and  $\nu_5$  is nicely described by these qualitative reasoning as well.

Now if there is an isospin imbalance,  $\nu \neq 0$ , in the system (together with chiral imbalance,  $\mu_5 \neq 0$ , hence, we suppose that other chemical potentials are zero,  $\mu = \nu_5 = 0$ ), then the situation is drastically different.

<sup>6</sup>In the chiral limit, the dynamical quark mass  $M$  is the order parameter of the CSB phase.

<sup>7</sup>Note that all phase portraits of Fig. 1 as well as some of the following diagrams are indeed the cross sections of the full phase diagram of the model under the constraint that at least one of the four chemical potentials is zero. In these cases it is enough to consider the phase portrait only at positive values of chemical potentials. It is a consequence of the fact that if one of the chemical potentials is zero, then the TDP (33) is an even function with respect to each of the remaining nonzero chemical potentials. So in each phase diagram of Fig. 1 only the regions with  $\mu_5 > 0$  are prepared.

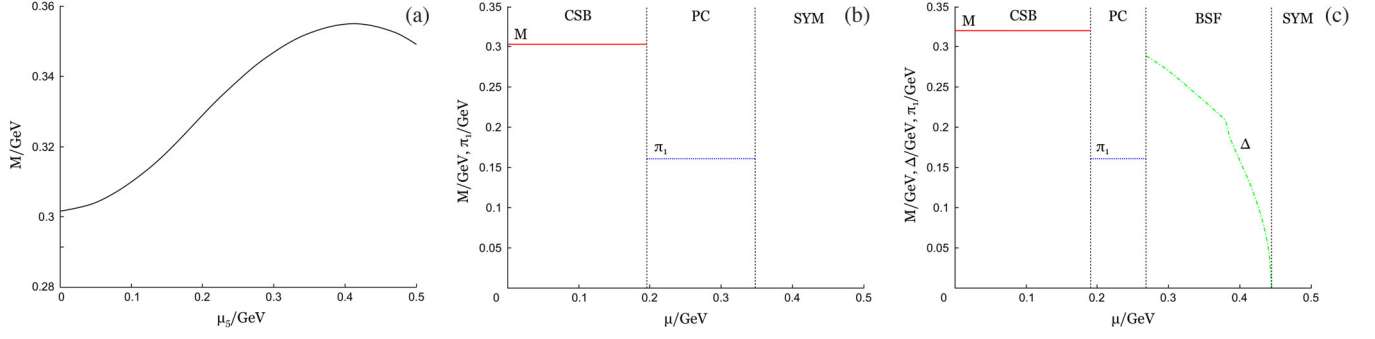


FIG. 2. The behaviors of condensates vs chemical potentials: (a)  $M$  as a function of  $\mu_5$  at  $\nu_5 = 0.1$  GeV,  $\mu = \nu = 0$  GeV. (b)  $M$  and  $\pi_1$  as a functions of  $\mu$  at  $\nu = 0$ ,  $\nu_5 = 0.25$  GeV and  $\mu_5 = 0.5$  GeV (c)  $\Delta$ ,  $\pi_1$  and  $M$  as a functions of  $\mu$  at  $\nu = 0$ ,  $\nu_5 = 0.2$  GeV and  $\mu_5 = 0.5$  GeV. The notations are the same as in Fig. 1.

In this case, to obtain the  $(\nu, \mu_5)$ -phase portrait of the massless two-color NJL model (1) [see in Fig. 1(b)], it is enough to apply, without any numerical calculations, to the phase diagram of Fig. 1(a) the dual  $\mathcal{D}_3$  transformation. The corresponding mechanism is described in Sec. III C, so we should change in Fig. 1(a)  $\nu_5 \rightarrow \nu$  and CSB  $\rightarrow$  charged PC. As a result, we have a phase portrait of Fig. 1(b). (Recall that the particular case of this diagram, when  $\nu > 0$  and  $\mu = \nu_5 = \mu_5 = 0$ , was discussed in Ref. [41], where it was established that at the points of the  $\nu$  axis of the diagram the charged PC phase is arranged at least for  $\nu < \Lambda$ . It was known that the order parameter of this phase, i.e., the charged pion condensate  $\pi_1$ , is increased if isospin density, i.e., isospin chemical potential, grows. It turns out that the pion condensate is also an increasing function vs  $\mu_5$ . It is an extremely surprising feature that  $\mu_5$  completely changed gears and, once isospin density is nonzero, start to catalyze charged pion condensation phenomenon instead of chiral symmetry breaking one. It is a consequence of the fact that in this case the condensate  $\pi_1$  is the  $\mathcal{D}_3$  mapping of the chiral condensate  $M$  of the CSB phase in Fig. 1(a). Hence, for the charged PC phase of Fig. 1(b) the plot of its order parameter  $\pi_1$  vs  $\mu_5$  at, e.g., fixed  $\nu = 0.1$  GeV can be obtained from Fig. 2(a) by two simple replacements,  $M \rightarrow \pi_1$  and  $\nu_5 = 0.1$  GeV  $\rightarrow \nu = 0.1$  GeV, etc. So in this particular case when  $\mu_5 \neq 0$ ,  $\nu \neq 0$  but  $\mu = \nu_5 = 0$ , the chiral imbalance  $\mu_5$  serves as a factor that catalyses (or enhances) the spontaneous breaking of the isospin  $U(1)_{I_3}$  symmetry, which manifests itself (without  $\mu_5$ ) even at  $\nu > 0$ ,  $\mu = \nu_5 = \mu_5 = 0$ .

Now let us make a couple of comments on the chiral limit and the current quark masses. Figures 1 have been shown in the chiral limit, i.e., at zero current quark mass  $m_0$ . At the physical point, at physical value of the current quark mass, the  $(\nu_5, \mu_5)$ -phase diagram of Fig. 1(a) would be the same, whereas the  $(\nu, \mu_5)$ -phase portrait of Fig. 1(b) would slightly change. One can see that pion condensation in Fig. 1(b) starts at infinitesimally small values of isospin chemical potential  $\nu$  in the chiral limit. In this case pion mass is zero and isospin density becomes nonzero at

infinitesimally small values of isospin chemical potential. In the physical point, i.e., at physical pion mass, isospin density emerges at isospin chemical potential  $\nu$  reaching the value of half of the pion mass, so one would see a small region of CSB phase at  $\nu < m_\pi/2$  and only at  $\nu > m_\pi/2$  charged PC phase sets in. So the  $\mu_5$  catalysis of chiral symmetry breaking will be switched to the catalysis of charged PC phenomenon at  $\nu = m_\pi/2$ , so overall the picture would stay the same.

Finally, if we are going to consider the phase structure of the two-color NJL model (1) in the chiral limit and in the case when  $\mu$ - and  $\mu_5$ -chemical potentials are nonzero but  $\nu = \nu_5 = 0$ , it is sufficient to perform the  $\mathcal{D}_2$ -dual transformation of the phase portrait of Fig. 1(a), or, alternatively, the  $\mathcal{D}_1$ -dual transformation of the phase portrait of Fig. 1(b). The results of these dual mappings is the  $(\mu, \mu_5)$ -phase diagram of Fig. 1(c), in which for the whole range of values of chemical potentials the baryon superfluid phase is arranged. The order parameter  $|\Delta|$  of this phase is also an increasing function vs  $\mu_5$  and/or  $\mu$  (it is clear after dual  $\mathcal{D}_2$  transformation of Fig. 2(a), i.e., replacing there  $M \rightarrow |\Delta|$  and the constraint  $\nu_5 = 0.1$  GeV  $\rightarrow \mu = 0.1$  GeV). Hence, in this region of chemical potentials the  $\mu_5$  catalyses/increases the BSF phase and spontaneous breaking of the baryon  $U(1)_B$  symmetry. The fact that  $\mu \neq 0$  leads to diquark condensation is natural and well known, whereas the same effect on phenomenon of diquark pairing by chiral imbalance is rather curious. This catalysis effect could be comprehended just by arguments of pairing on the Fermi surface, with the following qualitative arguments.

One can see from Eq. (3) that the Fermi momenta of  $u_L$  and  $d_L$  quarks in this case, i.e., at  $\nu = \nu_5 = 0$ , are  $\mu_{u_L} = \mu + \mu_5$  and  $\mu_{d_L} = \mu - \mu_5$ . As a result, it is clear that the condensation of Cooper  $u_L d_L$  pairs and appearing of the BSF phase is possible, in particular, both at  $\mu \neq 0$ ,  $\mu_5 = 0$  and at  $\mu = 0$ ,  $\mu_5 \neq 0$ . But in the last case we have from Eq. (3) that  $\mu_{u_L} = \mu_5$  and  $\mu_{u_R} = -\mu_5$ , i.e., an equal possibility for the condensation of the  $\bar{u}_R u_L$  pairs and generation of the CSB phenomenon. However, if both  $\mu \neq 0$  and  $\mu_5 \neq 0$ , then Fermi energies of  $u_L$  and  $d_L$  quarks

are equal (see above), which favors the formation of  $u_L d_L$  Cooper pairs, but  $\mu_{u_L} = \mu + \mu_5$  and  $\mu_{u_R} = \mu - \mu_5$ . So there is a mismatch in the Fermi surfaces of  $\bar{u}_R$  and  $u_L$  quarks which obstructs the formation of the Cooper  $\bar{u}_R u_L$  pairs. This allows us to say that, at  $\mu \neq 0$  and  $\mu_5 \neq 0$ , the formation of the BSF phase is preferable to the generation of the CSB phenomenon. Finally, we see that Fermi energies of  $u_L$  and  $d_L$  quarks (recall, in this case they are  $\mu + \mu_5$ ) are a growing vs  $\mu_5$  quantities, hence the order parameter  $|\Delta|$  of the BSF phase also increases with  $\mu_5$ , i.e., there is a catalysis of the BSF by chiral imbalance  $\mu_5$ .

So from the whole picture of the phase structure of chirally imbalanced,  $\mu_5 \neq 0$ , two-color quark matter that has another additional chemical potential, one can infer the following inherent characteristics of  $\mu_5$ . Chiral imbalance  $\mu_5$  enhances/catalyses any symmetry breaking phenomena realized in the system when it is under the influence of only this additional chemical potential. For example, if only  $\mu \neq 0$ , then baryon  $U(1)_B$  symmetry is broken spontaneously (diquarks have a nonzero condensate  $|\Delta|$ ) and  $\mu_5$  enhances just this effect. If there is a nonzero isospin imbalance in the system (only  $\nu \neq 0$ ) and charged PC phenomenon is observed in such a quark matter at  $\mu_5 = 0$ , then nonzero  $\mu_5$  (together with nonzero  $\nu$ ) enhances just the charged PC phenomenon as well as the spontaneous isospin  $U(1)_{I_3}$  symmetry breaking. Finally, if two-color quark matter is characterized by chiral isospin imbalance, only  $\nu_5 \neq 0$ , then at  $\mu_5 = 0$  the axial isospin (or chiral)  $U(1)_{AI_3}$  symmetry is broken spontaneously, CSB phase is realized in the system and quarks acquire dynamically a nonzero mass  $M$ . And in this case the nonzero  $\mu_5$  catalyses/enhances just this effect. So one can say that chiral imbalance  $\mu_5$  is a *universal catalyzer* for every phenomena in two color quark matter. But in this case it cannot trigger any phenomenon itself, it only enhances the phenomenon picked by other conditions of the medium.

Let us also stress that in its effect on the phase diagram  $\mu_5$  mimics other chemical potentials and in a way it is like chameleon, which assumes the color of the environment, it enhances the phenomena that are equally enhanced by other chemical potentials. For example, in Fig. 1(c) if  $\mu \neq 0$  when one goes along the  $\mu$  axis as well as one goes along  $\mu_5$  one (as long as even if small but  $\mu \neq 0$ ) the diquark condensate increases. So if only  $\mu \neq 0$  even if has small value then  $\mu_5$  can take the role of  $\mu$  and enhance diquark condensate quite dramatically. The universal catalyzer feature of chiral imbalance  $\mu_5$  is a manifestation of, as we will see below, chameleon property of  $\mu_5$ .

Although quite surprising and curious, this whole picture is the direct consequence of the dual properties of the phase diagram. At  $\mu_5 = 0$  the  $(\mu, \nu, \nu_5)$ -phase diagram of the two-color NJL model (1) is highly symmetric due to the dualities (see in Ref. [41]), and the expansion of this phase diagram to nonzero values of chiral chemical potential is also highly symmetric (see in Sec. III B) and possesses this

high dual symmetry as well. Now, for example, if one imagines the full  $(\mu, \nu, \nu_5, \mu_5)$ -phase diagram as a cube elongated to the  $\mu_5$  direction, then one can pick three facets of this phase diagram, namely  $(\nu_5 = 0$  and  $\nu = 0)$ ,  $(\nu = 0$  and  $\mu = 0)$  and  $(\mu = 0$  and  $\nu_5 = 0)$ , these facets are  $(\mu, \mu_5)$ ,  $(\nu_5, \mu_5)$  and  $(\nu, \mu_5)$  cross sections considered above in Fig. 1. So due to preservation of dualities at  $\mu_5 \neq 0$ , these facets are dual to each other. If one knows the behavior of the phase structure in one of them, then the others are predetermined.

Let us now try to imagine that we have not performed any calculations and try to anticipate the phase structure. In principle, one could get a lot of hints that CSB is catalyzed by chiral imbalance  $\mu_5 \neq 0$  and  $\nu_5 \neq 0$  in the whole plane  $(\nu_5, \mu_5)$  of Fig. 1(a). First, one knows that it was shown separately for each chiral chemical potential, and also it was bolstered by qualitative pairing arguments. Second, these arguments are easily generalized to the case of both simultaneously nonzero  $\mu_5$  and  $\nu_5$ . Then dualities dictate that chiral imbalance  $\mu_5$  leads to the catalysis of charged pion condensation at  $\nu \neq 0$ , see Fig. 1(b), and that it catalyzes diquark condensation at  $\mu \neq 0$ , see Fig. 1(c). So if it is obtained that chiral imbalance  $\mu_5$  catalyzes some phenomenon in some cross section of the full phase diagram, then the other phenomena are catalyzed by  $\mu_5$  in dually conjugated cross sections. The feature of chiral imbalance  $\mu_5$  of having the chameleon property is a consequence of dual properties of the full phase diagram of the model.

## B. Chemical potential $\mu_5$ is a universal catalyzer

In this section let us separately consider the situation when basic chemical potentials,  $\mu$ ,  $\nu$  and  $\nu_5$ , (dually-connected) reaches only rather moderate values. Let us first commence with the situation when only two of them are nonzero. Specifying the meaning of the moderate values scenario one should say that in this case it works when at least one of these chemical potentials is smaller than 0.2 GeV. Now let us, for instance, first consider the quark matter with nonzero baryon density,  $\mu \neq 0$ , and isospin imbalance,  $\nu \neq 0$ , and without chiral imbalances, i.e.,  $\mu_5 = \nu_5 = 0$ . Recall that in the particular case when there is only isospin imbalance in the system, i.e.,  $\mu = \mu_5 = \nu_5 = 0$ , and  $\nu \neq 0$ , then the charged pion condensation is realized [see in Fig. 1(b)], and if  $\mu \neq 0$  this passes to a ribbon of charged PC phase at rather large  $\nu$  at  $(\mu, \nu)$ -phase diagram [see Fig. 3(a)]. But if the isospin imbalance is not so large ( $\nu$  smaller than 0.2 GeV), then at baryon density corresponding to the value  $\mu = \nu$  the phase transition to BSF phase takes place and diquark condensation appears in the system, and at rather large  $\mu > \nu$  there is a whole band of BSF phase [see Fig. 3(a)]. One could behold that in this regime the largest chemical potential defines the phase structure: if it is baryon chemical potential then diquark condensation prevail, and if it is isospin one then charged pion condensation takes over.

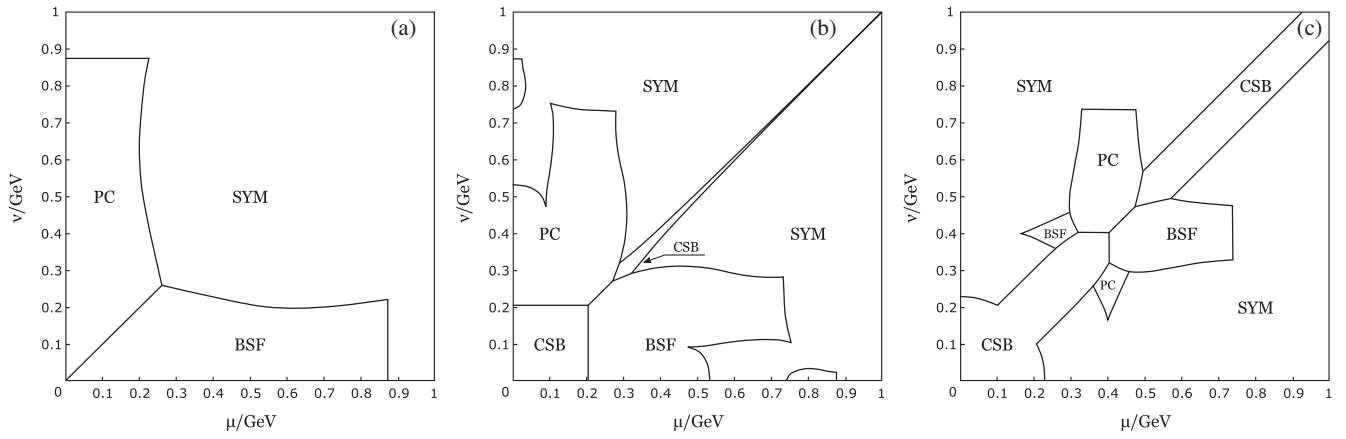


FIG. 3.  $(\mu, \nu)$ -phase diagrams at: (a)  $\mu_5 = \nu_5 = 0$  GeV. (b) at  $\mu_5 = 0$  GeV,  $\nu_5 = 0.2$  GeV. (c) at  $\mu_5 = 0$  GeV,  $\nu_5 = 0.4$  GeV. The notations are the same as in Fig. 1.

Now, if one increases the value of chiral chemical potential  $\mu_5$ , which was equal to zero in the discussion above, then the  $(\nu, \mu)$ -phase diagram of Fig. 4(a) at  $\mu_5 = 0.4$  GeV and  $\nu_5 = 0$  could be obtained by numerical analysis, and one can note that in the discussed regime the phases and the phase transition do not alter at all (see in Fig. 4(a) the region of small values,  $<0.2$  GeV, of  $\mu$  or  $\nu$ , the other regions will be discussed later).

Now let us turn our sight to the other cross sections of the full phase diagram containing chiral chemical potential  $\mu_5$ . In particular, it is possible to consider how the  $(\nu, \mu_5)$ -phase diagram of Fig. 1(b), which is drawn under the condition  $\mu = \nu_5 = 0$ , changes when one increases  $\mu$  up to 0.2 GeV ( $\nu_5$  is still equal to zero). Or, in other words, it is an expansion of the cross section of fixed  $\mu$  to nonzero values of  $\mu_5$ . Numerical analysis shows that in this case the typical  $(\nu, \mu_5)$ -phase portrait of the model looks like the one of Fig. 5(a), which is depicted for fixed  $\mu = 0.1$  GeV. It means that in these phase portraits at  $\nu < \mu$  the BSF phase is arranged, but at  $\nu > \mu$  one can see the charged PC phase.

Interestingly enough that the transition line between the PC and BSF phases is a straight line (it does not depend on the value of  $\mu_5$ ), and the phase in this case is entirely chosen by the relation between values of  $\mu$  and  $\nu$  chemical potentials. It is in full agreement with the fact that for moderate  $\mu$  and  $\nu$  values the phase transitions at the  $(\nu, \mu)$ -phase diagram of Fig. 4(a) was not influenced a lot by chiral chemical potential  $\mu_5$ . Bearing in mind that the section of  $\mu_5 = 0.4$  GeV in Fig. 5(a) is the section  $\mu = 0.1$  GeV in Fig. 4(a), one could easily comprehend that the phase transition in Fig. 5(a) is at  $\nu = \mu$  and it shifts to larger values of  $\nu$  if quark number chemical potential  $\mu$  is increased. Apart from the fact that the transition line in Fig. 5(a) between the PC and BSF phases is a straight line, let us elaborate more on the effect of chiral  $\mu_5$ . As for  $\mu_5 = 0$  as well as for  $\mu_5 \neq 0$  the same phase structure is observed, i.e., at  $\nu < \mu$  ( $\nu > \mu$ ) the BSF (the charged PC) phase is realized, but the order parameters of these phases are growing functions vs  $\mu_5$ , and the increase is quite dramatic as one can see in Fig. 2(a). From all these one can conclude that for this set of

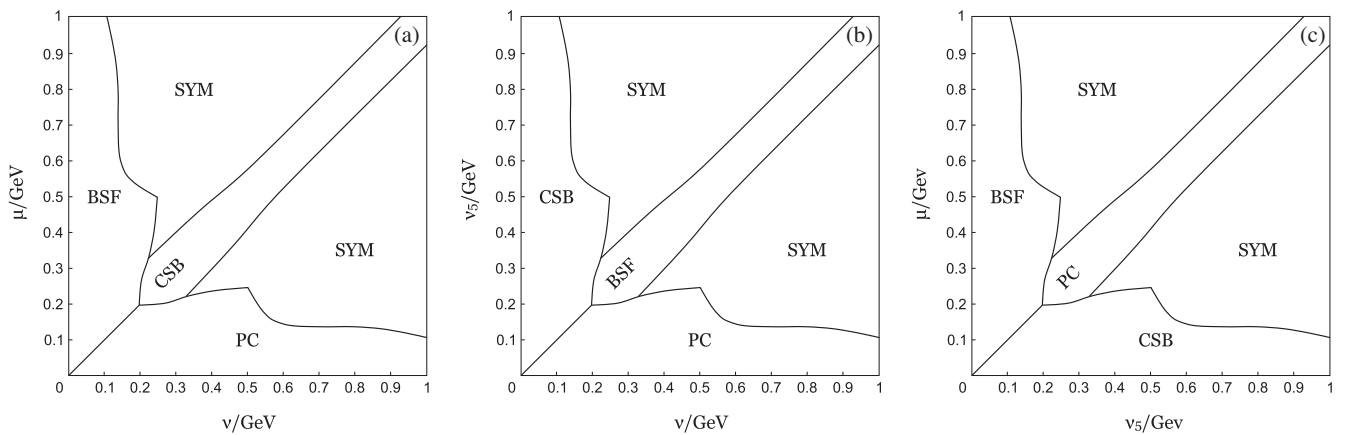


FIG. 4. Dually conjugated phase portraits: (a)  $(\nu, \mu)$ -phase diagram at  $\mu_5 = 0.4$  GeV,  $\nu_5 = 0$  GeV. (b)  $(\nu, \nu_5)$ -phase diagram at  $\mu_5 = 0.4$  GeV,  $\mu = 0$  GeV. It is a  $\mathcal{D}_2$  mapping of Fig. 4(a). (c)  $(\nu_5, \mu)$ -phase diagram at  $\mu_5 = 0.4$  GeV,  $\nu = 0$  GeV. It is a  $\mathcal{D}_3$  mapping of the diagram Fig. 4(a). The notations are from Fig. 1.

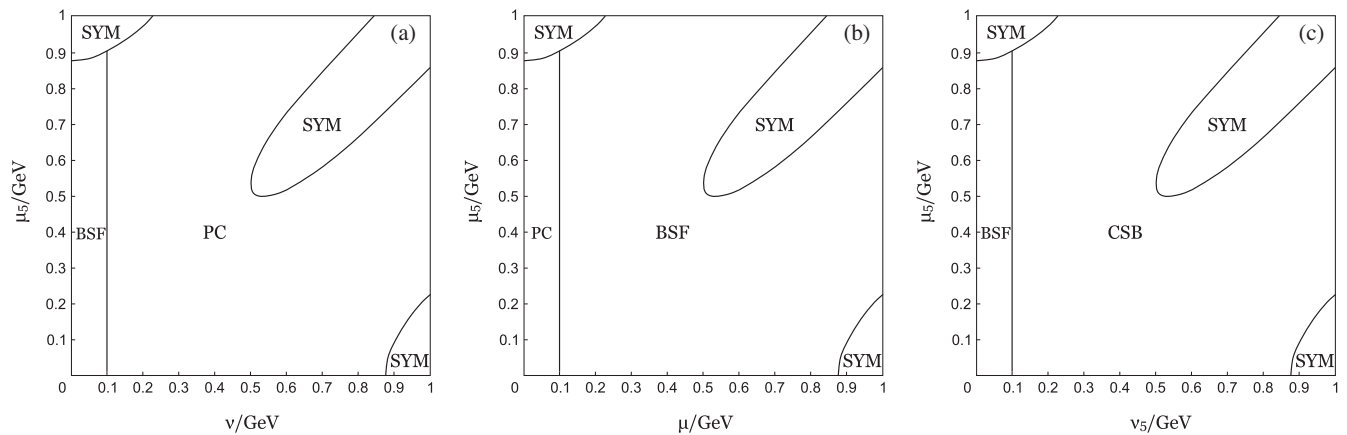


FIG. 5. Dually conjugated phase portraits: (a)  $(\nu, \mu_5)$ -phase diagram at  $\mu = 0.1$  GeV,  $\nu_5 = 0$  GeV. (b)  $(\mu, \mu_5)$ -phase diagram at  $\nu_5 = 0$ ,  $\nu = 0.1$  GeV. It is a  $\mathcal{D}_1$  mapping of Fig. 5(a). (c)  $(\nu_5, \mu_5)$ -phase diagram at  $\mu = 0.1$  GeV,  $\nu = 0$  GeV. It is a  $\mathcal{D}_3$  mapping of Fig. 5(a). The notations are from Fig. 1.

chemical potentials the  $\mu_5$  catalyzes (or enhances) the phenomena observed at  $\mu_5 = 0$ . This feature was already noticed and discussed above in Sec. IV A for the particular case of two nonzero chemical potentials (one of them is  $\mu_5$ ).

Applying, for example, to the phase diagram of Fig. 5(a) the dual  $\mathcal{D}_1$  or dual  $\mathcal{D}_3$  mappings, etc, one can obtain the  $(\mu, \mu_5)$ -phase portrait at fixed  $\nu_5 = 0$  and  $\nu = 0.1$  GeV [see in Fig. 5(b)], or the  $(\nu_5, \mu_5)$ -phase portrait [see in Fig. 5(c)] at  $\mu = 0.1$  GeV,  $\nu = 0$ , respectively. Since under the dual transformations the properties of the order parameters are not changed, we can conclude that for these particular sets of the basic chemical potentials  $\mu$ ,  $\nu$ , and  $\nu_5$  the order parameter of each nonsymmetrical phase is indeed an increasing function vs  $\mu_5$ , i.e., the chemical potential  $\mu_5$  is a catalyst of the phase structure observed at  $\mu_5 = 0$ .

Now let us turn our gaze to the phase structure of the model in the case of three nonzero basic chemical potentials  $\mu$ ,  $\nu$  and  $\nu_5$  (and first keep the value of chiral imbalance  $\mu_5$  equal to zero) in the regime of moderate values, talking more specifically in this case at least two of them should be smaller than 0.2 GeV. In this case the  $(\mu, \nu)$ -phase diagram at  $\nu_5 = 0.2$  GeV is depicted in Fig. 3(b) and one can see that if  $\mu = 0$  then at  $\nu < \nu_5 = 0.2$  GeV the system is in the CSB phase as it should be since there is rather large chiral imbalance  $\nu_5$ . Then, if the value of  $\nu$  is increased and reaches the value of  $\nu = \nu_5 = 0.2$  GeV, then the phase transition to the charged PC phase takes place and at  $\nu > \nu_5 = 0.2$  GeV the charged pion condensation only solidifies. Now let us take  $\nu = 0$ . As it clear from Fig. 3(b), at  $\mu < \nu_5 = 0.2$  GeV there is CSB phase due to the same reasons. But at  $\mu = \nu_5 = 0.2$  GeV the phase transition to BSF phase occurs, and diquark condensation is prevailing. In the latter example, if one assume that  $\nu \neq 0$  but less than  $\nu_5 = 0.2$  GeV then nothing changes and the phase transition occurs at exactly the same point  $\mu = \nu_5 = 0.2$  GeV, so one can conclude that if  $\nu < \mu, \nu_5$  then it does not influence much the phase structure at all. Now, if

$\nu > \nu_5 = 0.2$  GeV then one can see in Fig. 3(b) that at increasing  $\mu$  the charged PC phase continues to dominate up to the value of  $\mu = \nu$ , and  $\nu_5$  does not play almost any role here.

So, at  $\mu_5 = 0$  one can characterize the general picture (in the case of moderate basic chemical potential values) in the following manner. (i) Each basic chemical potential (i.e.,  $\mu$ ,  $\nu$ , or  $\nu_5$ ) is in one-to-one correspondence with one of CSB, BSF, or charged PC phases, i.e., to a corresponding condensation and symmetry breaking patterns. For example,  $\mu$  corresponds to BSF phase,  $\nu$ —to charged PC, and  $\nu_5$ —to CSB phase. (ii) The largest chemical potential sets the corresponding phase that occupies the system. Hence, if the triplet of chemical potentials  $\mu$ ,  $\nu$ , and  $\nu_5$  has moderate values and  $\mu_5 = 0$ , then to get the phase structure one could find just the chemical potential with the highest value, and it defines the phase that is realized in the system. The other two do not play a significant role here. This picture unfolds only in the regime of moderate values of basic chemical potentials (recall, by this regime we mean here that at least two from three basic chemical potentials have values smaller than 0.2 GeV). Let us stress that we have chosen the value  $\nu_5 = 0.2$  GeV in Fig. 3(b) on purpose (based on it one can easily envisage, for example, the phase diagram at  $\nu_5 = 0.1$  GeV), since it is a borderline value and one could see that if  $\mu_5$  is also small (in Fig. 3(b)  $\mu_5 = 0$ ), then this picture holds even if values of  $\mu$  and  $\nu$  can reach almost 0.3 GeV, even slightly out of the scope that we called moderate values. But if the values of  $\mu$ ,  $\nu$ , and  $\nu_5$  lies inside the moderate regime, i.e., at least two of them are less than 0.2 GeV, then this concise and elegant picture unhesitatingly persists to any values of chiral chemical potential  $\mu_5$ , one could see this in Fig. 5.

Now let us allow chiral chemical potential  $\mu_5$  to be nonzero in the case of three nonzero basic chemical potentials  $\mu$ ,  $\nu$  and  $\nu_5$ . This could be contemplated as the expansion of the phase diagram portrayed in Fig. 3(b),

where  $\mu_5$  is equal to zero, to nonzero values of  $\mu_5$ . In the most concise way it could be formulated that in the regime of moderate values discussed above the phases and phase transitions stay at their places and just condensates are enhanced, so chiral imbalance  $\mu_5$  catalyses all three phases. It could be demonstrated probably in the most convenient way by making the value of the fourth chemical potential nonzero, namely  $\nu_5$  in Fig. 5(a) and increasing its value. If  $\nu_5$  is smaller than  $\mu = 0.1$  GeV then at  $\nu < 0.1$  GeV the BSF phase is intact and continues to occupy the whole region of  $\nu < 0.1$  GeV and the whole phase diagram in Fig. 5(a) is unchanged and chiral chemical potential  $\mu_5$  catalyzes BSF and PC phases. But if the value of  $\nu_5 > \mu = 0.1$  GeV, then the whole region of  $\nu < \nu_5$  GeV is occupied by CSB phase and chiral chemical potential  $\mu_5$  starts to catalyze chiral condensation in the region  $\nu < \nu_5$  GeV. And if  $\nu > \nu_5$  GeV it continues to catalyze charged pion condensation phenomenon. Let us also note here that the phase diagram presented in Fig. 5(a) (recall that this figure is shown in the chiral limit  $m_0 = 0$ ) does not change in the physical point, when one takes physical nonzero value of current quark mass, since the value of the quark number chemical potential  $\mu$  is already larger than half of pion mass.

Concluding, let us reiterate the phase picture in the regime of moderate and rather low values of basic chemical potentials in a concise form. It can be characterized in the following manner. Each basic chemical potential is in one-to-one correspondence with one of the possible nontrivial phases of the model (charged PC, BSF, or CSB), as well as with its order parameter/condensate (isospin chemical potential  $\nu$  corresponds to the charged PC phase, quark number chemical potential  $\mu$ —to the BSF phase, etc) and the largest chemical potential fully determines the phase that occupies the system. Chiral chemical potential  $\mu_5$  does not influence the phase transition features, in other words  $\mu_5$  does not choose any phase but it *catalyzes* the phases, enhancing their condensates, picked by basic chemical potentials.

## C. The ability of $\mu_5$ to trigger various phases

### 1. The case when two of $\mu$ , $\nu$ and $\nu_5$ have rather large values

Now let us switch gears a little bit and turn our attention to the regime when basic chemical potentials  $\mu, \nu, \nu_5$  has rather large values. It is reasonable to start with the situation when only two of chemical potentials  $\mu, \nu, \nu_5$  are nonzero and have rather large values and the remaining chemical potential is equal to zero.

So take a look at Fig. 3(a), where  $(\mu, \nu)$ -phase diagram at  $\mu_5 = 0$  and  $\nu_5 = 0$  is depicted. It does not contain any region with CSB phase. Then, with increasing  $\mu_5$ , when it reaches the critical value  $\mu_{5c} \in 0.15 \div 0.2$  GeV, on the  $(\mu, \nu)$ -phase diagram, which is under the constraint  $\nu_5 = 0$ ,

the band of CSB phase *suddenly* appears along the straight line  $\mu = \nu$ , when these chemical potentials are larger than  $0.2$  GeV. The typical  $(\mu, \nu)$ -phase diagram at  $\nu_5 = 0$  and  $\mu_5 = 0.4$  GeV is given in Fig. 4(a), which is obtained by numeric calculation. And one can see in this figure that for the values of  $\mu \approx \nu$  the band of the CSB phase is realized. This leads to curious consequences, for example, in the dense quark matter with rather considerable isospin imbalance when  $\mu \approx \nu$ , if one has nonzero chiral imbalance  $\mu_5$  then increasing the baryon density and keeping the ratio of baryon and isospin chemical potentials the same, one could not restore chiral symmetry even at very large baryon density. As a rule (if there is no chiral imbalance), either keeping isospin asymmetry nonzero or vanishing, chiral symmetry gets restored at rather large values of baryon chemical potential.

One can also recall that the same pattern was observed in the case of nonzero  $\nu_5$  at  $\mu_5 = 0$ . For example, the  $(\mu, \nu)$ -phase diagram at  $\nu_5 = 0.4$  GeV and  $\mu_5 = 0$  is presented in Fig. 3(c). (It is also interesting to note that, like any  $(\mu, \nu)$ -phase diagrams of the model at fixed values of  $\nu_5$  and  $\mu_5$ , the phase portraits in Fig. 3 are self-dual with respect to the action of the duality- $\mathcal{D}_1$  transformation (30) on them, i.e., charged PC and BSF phases are located on the figures mirror-symmetrically relative to the straight line  $\mu = \nu$ .) Comparing the diagrams of Figs. 4(a) and 3(c), one could notice that the discussed above band of CSB phase does not depend on which chiral chemical potential is nonzero,  $\nu_5$  or  $\mu_5$ . These CSB-bands coincide in the whole range of values of  $\mu_5$  and  $\nu_5$ . The presence of these bands can serve as an additional indication of the tendency that chiral imbalance promotes chiral symmetry breaking. But in this case the promotion is qualitatively different from the one discussed above, and the chiral imbalances *genuinely generates* chiral symmetry breaking and not just enhance (or catalyze) the CSB triggered by other factors.

This behavior, i.e., the generation of band-shaped domain of CSB phase, can be easily qualitatively understood. As it follows from Eq. (3), for nonzero values of  $\nu_5$  in the region  $\mu \approx \nu$  and  $\mu_5 = 0$  the Fermi momenta of  $d_L$  and  $d_R$  quarks are  $\mu_{d_L} = \mu - \nu - \nu_5 \approx -\nu_5$  and  $\mu_{d_R} = \mu - \nu + \nu_5 \approx +\nu_5$ , respectively. So the condensation of the  $\bar{d}_L d_R$  pairs is possible and chiral symmetry is broken down. For nonzero  $\mu_5$  and  $\nu_5 = 0$  the situation is similar, in this case the Fermi momenta are  $\mu_{d_L} \approx \mu_5$  and  $\mu_{d_R} \approx -\mu_5$ , and the condensation of, for example,  $\bar{d}_R d_L$  pairs is possible, and CSB phase is realized as well. The larger  $\mu_5$  or  $\nu_5$ , the stronger the effect and it can be realized in the broader band when the cancellation of  $\mu$  and  $\nu$  is less pronounced.

Now let us contemplate the different setup, namely the  $(\nu, \nu_5)$ -phase diagram and the way how it is affected by chiral imbalance  $\mu_5$  at  $\mu = 0$ . It is fairly easy to obtain this phase diagram, applying the  $\mathcal{D}_2$ -duality mapping to the corresponding  $(\mu, \nu)$ -phase diagram at the same value of  $\mu_5$  and at  $\nu_5 = 0$ . For example, the  $(\nu, \nu_5)$ -phase diagram at



$\mu_5 = 0.4$  GeV and  $\mu = 0$  is depicted in Fig. 4(b), where the band of BSF phase appears around the line  $\nu = \nu_5$  when these chemical potentials are large enough,  $> 0.2$  GeV. The diagram of Fig. 4(b) is indeed a  $\mathcal{D}_2$ -duality mapping of Fig. 4(a). Moreover, the BSF band *suddenly* appears on these  $(\nu, \nu_5)$ -phase diagrams with  $\mu = 0$  even at smaller values of  $\mu_5 > \mu_{5c} \in 0.15 \div 0.2$  GeV. So in this case the situation drastically changes and chiral imbalance  $\mu_5$  generates diquark condensation instead of chiral symmetry breaking. Exactly the same band form of the BSF phase can be observed at the  $(\nu, \nu_5)$ -phase diagram with  $\mu_5 = 0$  at corresponding nonzero values of baryon (quark number) chemical potential  $\mu$ . One could easily envisage it by applying the  $\mathcal{D}_2$ -duality mapping to Fig. 3(c) and one can see that the behavior of these band-shaped regions, for  $\mu \neq 0, \mu_5 = 0$  and  $\mu = 0, \mu_5 \neq 0$ , are exactly the same. As for the baryon density,  $\mu \neq 0$ , it is expected and natural to induce diquark condensation, it is small wonder that at some regime the chemical potential  $\mu$  leads to diquark condensation (it does even in the simplest case of only  $\mu \neq 0$ ) but the fact that chiral chemical potential  $\mu_5$  is doing the same job is surprising enough, even more surprising that it does it in exactly the same way as baryon one. Now let us reflect on the mechanism of emergence of the band-shaped region of BSF phase in  $(\nu, \nu_5)$ -diagrams of Fig. 4(b) type. The Fermi energies in this case of  $\nu = \nu_5$  are  $\mu_{u_R} \approx \mu - \mu_5$ ,  $\mu_{d_R} \approx \mu - \mu_5$ . Hence, if  $\mu_5 = 0$  and  $\mu \neq 0$  then the creation of Copper pairs of the form  $u_R d_R$  is quite possible, and their condensation leads to the appearance of the band-shaped BSF phase along the line  $\nu_5 \approx \nu$  of the  $(\nu, \nu_5)$ -phase diagram at some fixed  $\mu$ . But in the case of the  $(\nu, \nu_5)$ -phase diagram of Fig. 4(b) type, when  $\mu = 0$  and  $\mu_5 \neq 0$ , one can witness that the creation of Copper pairs of the form  $\bar{u}_R \bar{d}_R$  is possible at  $\nu_5 \approx \nu$ , also leading to the strip of the BSF phase in Fig. 4(b).

Now consider the influence of chiral chemical potential  $\mu_5$  on the dense quark matter with chiral isospin imbalance, i.e., on the  $(\nu_5, \mu)$ -phase diagram. The particular diagram of this kind is presented in Fig. 4(c) at  $\nu = 0$  and  $\mu_5 = 0.4$  GeV. And it is obtained (without any numerical calculations) simply by the action, e.g., of the  $\mathcal{D}_3$ -dual mapping on the diagram of Fig. 4(a). It is clearly seen that in Fig. 4(c) the bandlike region of charged PC phase is spawned at  $\mu \approx \nu_5$ , and this phase is  $\mathcal{D}_3$ -dually conjugated to the bandlike CSB phase of Fig. 4(a). Also in this case interestingly enough that this phase completely coincides with the charged PC phase at the  $(\mu, \nu_5)$ -phase diagram at  $\mu_5 = 0$  and  $\nu = 0.4$  GeV, which is a  $\mathcal{D}_3$ -dual mapping of the diagram in Fig. 3(c). So in  $\mu \approx \nu_5$  environment chiral imbalance  $\mu_5$  fully takes a role of isospin  $\nu$  one and causes the charged PC to crop up. In this region of phase structure the effects of chiral imbalance  $\mu_5$  and isospin imbalance  $\nu$  is fully tantamount.

One can conclude that in the regime when values of basic chemical potentials  $\mu, \nu, \nu_5$  reach rather large values, the

influence of chiral imbalance  $\mu_5$  can be rather different, than just a universal catalyst for any pattern of symmetry breaking in the system. To support this statement, above we have considered in details the influence of  $\mu_5$  on the phase structure of the model for three particular sets of basic chemical potentials, (i)  $\nu_5 = 0$  but  $\mu, \nu > 0.2$  GeV, (ii)  $\mu = 0$  but  $\nu, \nu_5 > 0.2$  GeV, (iii)  $\nu = 0$  but  $\mu, \nu_5 > 0.2$  GeV. It turns out that at  $\mu_5 = 0$  as well as at a rather small vicinity of the zero point, the system is in the symmetrical phase for each set (i)-(iii) of chemical potentials (this conclusion is well illustrated by Fig. 3(a) and its dual conjugations). However, when  $\mu_5 > \mu_{5c}$ , the chiral imbalance  $\mu_5$  *induces* some symmetry breaking. In this case, depending on the conditions,  $\mu_5$  can assume either the role of baryon chemical potential and generate the diquark condensation [for the set (ii)], or isospin chemical potential and trigger charged PC [for the set (iii)], or chiral isospin chemical potential  $\nu_5$  and be a reason of CSB [for the set (i)]. One can say that the statement that the chiral imbalance  $\mu_5$  has a chameleon nature, i.e., it can pretend to be either chemical potential depending on the situation is supported once again. And here it does not just catalyze the symmetry breaking and enhance the corresponding condensate as in chiral symmetry breaking catalysis observed when only  $\mu_5 \neq 0$  [46], but *causes* the symmetry breaking to happen in the first place.

Let us reflect on the chiral imbalance  $\mu_5$  in terms of dualities and its ability to generate various phenomena. Chiral chemical potential  $\mu_5$  does not participate in the duality transformations, it only keeps the dualities of  $(\mu, \nu, \nu_5)$ -phase structure intact, i.e.,  $(\mu, \nu, \nu_5)$ -phase diagram at  $\mu_5 = 0$  and its expansion to nonzero chiral chemical potential  $\mu_5$  is highly symmetric due to dualities. This leads to the fact that one can shuffle the facets of the  $(\mu, \nu, \nu_5)$ -phase diagram and due to this the influence of  $\mu_5$  on various phenomena would be the same, since these facets are connected by duality transformations. So the influence of  $\mu_5$  on the  $(\mu, \nu, \nu_5)$ -phase structure is constrained by dualities and the chameleon nature of chiral chemical potential is inevitable and it is a consequence of dual properties of the phase diagram. The universality of effect of chiral chemical potential on various phenomena (the fact that  $\mu_5$  influence CSB, PC and BSF phases equally in various conditions) is inevitable and it is a consequence of dual properties of the phase diagram. For example, if one knows that at  $\mu_5 > \mu_{5c}$  chiral imbalance generates chiral symmetry breaking in dense quark matter with isospin imbalance,  $\mu \approx \nu$ , see Fig. 4(a), then one could use the duality and find out that chiral imbalance can generate diquark condensation (at  $\nu_5 \approx \nu$ ) and charged PC (at  $\mu \approx \nu_5$ ), as it is clear from Figs. 4(b) and 4(c), respectively.

## 2. Dense quark matter with isospin and both chiral imbalances: The case of nonzero $\mu, \nu, \nu_5$ , and $\mu_5$

Now let us discuss the most generic situation when besides nonzero chiral imbalance  $\mu_5$  all three chemical

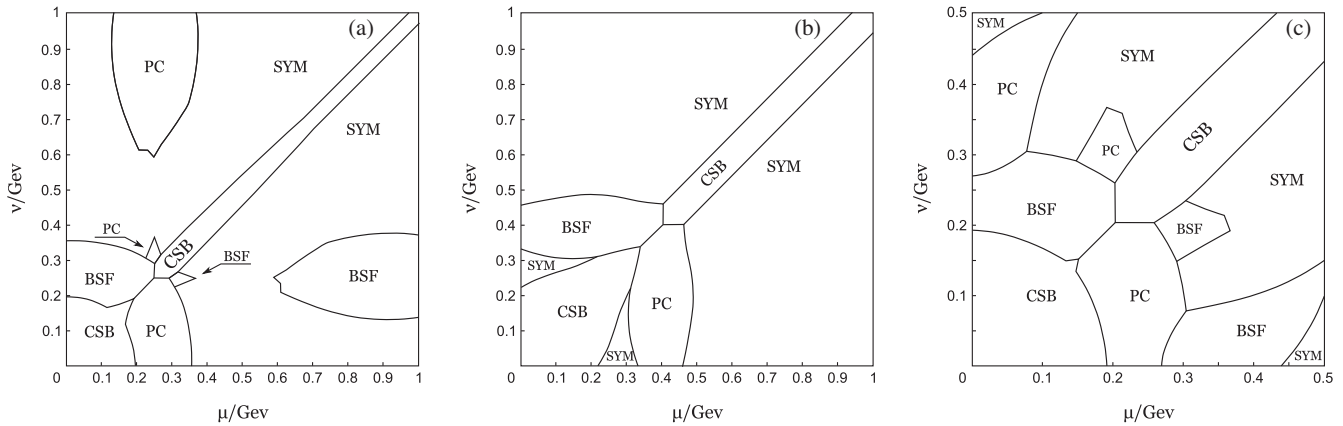


FIG. 6.  $(\mu, \nu)$ -phase diagrams: (a) at  $\nu_5 = 0.25$  GeV,  $\mu_5 = 0.5$  GeV, (b) at  $\nu_5 = 0.4$  GeV,  $\mu_5 = -0.3$  GeV, (c) at  $\nu_5 = 0.2$  GeV,  $\mu_5 = 0.5$  GeV. The notations are from Fig. 1.

potentials  $\mu, \nu, \nu_5$  are nonzero. This kind of general situation has been already considered in the regime of small and moderate values of  $\mu, \nu, \nu_5$  chemical potentials in Sec. IV B. In this section, let us turn our attention to the regime where these chemical potentials have rather large values.

To begin with, we are going to investigate what happens to the  $(\mu, \nu)$ -phase diagram at nonzero fixed values of  $\nu_5$ , if one starts to increase the value of chiral chemical potential  $\mu_5$ . In particular, the  $(\mu, \nu)$ -phase diagram in the cases with only one chiral imbalance, i.e., at different nonzero values of  $\mu_5$  and zero  $\nu_5 = 0$  and at  $\nu_5 \neq 0$  and  $\mu_5 = 0$ , has been already deliberated in detail in Sec. IV C 1. So first of all let us recall how the variation of chiral isospin  $\nu_5$  chemical potential value would be imprinted at the  $(\mu, \nu)$ -phase diagram in the case  $\mu_5 = 0$ . Several diagrams of this type are shown in Fig. 3. As it is clear from it (see also in Ref. [41]) and has been discussed above, if one increases  $\nu_5$  the boot-shaped elongated regions of charged PC and BSF phases at  $\mu \approx \nu_5$  and  $\nu \approx \nu_5$  are shifted to the larger values of  $\mu$  and  $\nu$ , respectively. This effect, for example, leads to the generation of charged PC phase at larger baryon density, the similar effect in three color case led to the generation of charged pion condensation in dense quark matter with chiral imbalance [38].

Now let us return to the discussion of the influence of chiral chemical potential  $\mu_5$  and recall in the first place that in the case of all four nonzero chemical potentials there is no symmetry of the TDP (33) of the form  $\mu \rightarrow -\mu$  or  $\mu_5 \rightarrow -\mu_5$  etc. and, for example, the cases  $\mu_5 > 0$  and  $\mu_5 < 0$  has to be considered separately. So, recall that in the most general case, one can consider various combinations,  $\mu > 0, \nu > 0$ , and  $\nu_5 > 0$  but the value of chiral imbalance  $\mu_5$  is of any sign, or  $\mu > 0, \nu > 0$ , and  $\mu_5 > 0$  and the sign of  $\nu_5$  is not fixed or any other combination [see the remark in the second paragraph below Eq. (33)].

Let us choose the former option, the one where basic chemical potentials  $\mu, \nu$ , and  $\nu_5$  are positive and  $\mu_5$  can be

of both signs, and first take the case of negative values of  $\mu_5$ . We would like to explore what effect chiral imbalance  $\mu_5$  leaves on the  $(\mu, \nu)$  diagram at fixed  $\nu_5 \neq 0$ . For example, to understand what would happen to Fig. 3(c) if one increases the value of chiral imbalance  $|\mu_5|$  provided that  $\mu_5 < 0$ , take a look at Fig. 6(b). There the influence of the  $\mu_5 = -0.3$  GeV [instead of  $\mu_5 = 0$  as in Fig. 3(c)] on the  $(\mu, \nu)$ -phase diagram at fixed  $\nu_5 = 0.4$  GeV is shown. As a result, one can see that the bootlike charged PC and BSF phases are shifted to the smaller values of  $\nu$  and  $\mu$  respectively, i.e., along the direction that they are elongated along. Let us note that it is a perpendicular direction to the one they shift when one increases  $\nu_5$ .

And at some rather large  $|\mu_5|$  the charged PC and BSF phases of  $(\mu, \nu)$ -phase diagram with some fixed  $\nu_5$  transfix the axes  $\mu$  and  $\nu$ , respectively [see Fig. 6(b)]. Hence, a rather interesting picture unfolds, i.e., one could see that at large enough values of chiral imbalances  $\nu_5$  and negative  $\mu_5$  the diquark condensation takes place in the region of phase diagram with rather small or zero baryon density,  $\mu = 0$ , whereas charged pion condensation is favored in the region of large baryon (quark number) density,  $\mu \neq 0$ , and small isospin chemical potential  $\nu$ .<sup>8</sup> Especially interesting is the feature of dense quark matter when at nonzero chiral imbalances,  $\nu_5 > 0$  and  $\mu_5 < 0$ , and zero isospin one,  $\nu = 0$ , the baryon chemical potential  $\mu$  is increased gradually [see, e.g., the movement along the line  $\nu = 0$  in Fig. 6(b)]. First, if  $\mu$  is zero or small then CSB phase is realized due to rather large chiral imbalance  $\nu_5$ , then at larger values of  $\mu$  the charged PC is triggered instead of diquark condensation. Due to a  $\mathcal{D}_1$ -self-duality of the  $(\mu, \nu)$ -phase

<sup>8</sup>All this is in drastic contrast to the regular behavior at zero chiral imbalances  $\nu_5$  and  $\mu_5$  [6–8, 12–21], or if only one of them is present, where BSF phase (charged PC phase) is generated when there is nonzero  $\mu$  (isospin imbalance  $\nu$ ), or if baryon chemical potential  $\mu$  (isospin chemical potential  $\nu$ ) has higher values than the other ones [41].

diagram of Fig. 6(b), a similar, but opposite, phenomenon occurs when at zero baryon chemical potential  $\mu = 0$  one increases the isospin one. It is clear from Fig. 6(b) that at moderate values of  $\nu$  less than 0.2 GeV chiral symmetry breaking predominates, due to chiral isospin imbalance  $\nu_5 > 0$ , but at larger values of  $\nu$ , instead of pion condensation that is usually promoted by isospin chemical potential, the diquark condensation develops in the system. The remarkable feature is that even at exactly zero baryon chemical potential  $\mu = 0$  the diquark condensation is prevailing in full swing.

Now let us consider the case  $\mu_5 > 0$ . Then with increase of the value of  $\mu_5$  the bootlike charged PC and BSF phases of the  $(\mu, \nu)$ -phase diagram (at some fixed  $\nu_5$  and  $\mu_5$ ) are shifted to opposite direction (compared to the case  $\mu_5 < 0$ ), i.e., to the larger values of  $\nu$  and  $\mu$ , respectively. For example, in Fig. 6(a) the  $(\mu, \nu)$ -phase diagram in the case  $\nu_5 = 0.25$  GeV and  $\mu_5 = 0.5$  GeV is depicted. [The value of  $\nu_5 = 0.25$  GeV, not  $\nu_5 = 0.4$  GeV as in Fig. 6(b), is taken for a change, and if needed one can easily envision the  $(\mu, \nu)$ -phase structure at  $\nu_5 = 0.4$  GeV and  $\mu_5 = 0.5$  GeV, where the charged PC and BSF phases would be shifted to the larger values of  $\nu$  and  $\mu$ , respectively, in comparison with the  $(\mu, \nu)$ -phase diagram of Fig. 3(c) at  $\nu_5 = 0.4$  GeV and  $\mu_5 = 0$ , exactly in the same way as the phase structure evolves at  $\nu_5 = 0.25$  GeV from Figs. 3(b)–6(a). We will discuss the additional reasoning apart from diversity and clarity for this choice below, now let us turn back to phase structure of Fig. 6(a).] While these bootlike PC and BSF phases are moved to larger values of  $\nu$  and  $\mu$  chemical potentials, there a new bootlike region of BSF (charged PC) phase appears from the small values of  $\nu$  ( $\mu$ ), see Fig. 6(a). In this case of  $\mu_5 > 0$  one can see that the diquark condensation could be triggered in the quark matter with zero baryon chemical potential  $\mu = 0$  as well.

Thus, the analysis of the phase diagrams in Fig. 6 allows us to draw a very interesting conclusion that in both cases, negative or positive values of  $\mu_5$ , even at zero baryon density,  $\mu = 0$ , in quark matter with an increase of  $\nu$ , a BSF phase can arise, which is *induced* in the system only in the presence of a rather large chiral asymmetry (large value of  $|\mu_5|$ ). From the diagrams in Fig. 6, a dually- $\mathcal{D}_1$  conjugate conclusion also follows: if the isospin density in quark matter is zero,  $\nu = 0$ , then with increasing of  $\mu$  in it, in the presence of a chiral asymmetry with a large value of  $|\mu_5|$ , a charged PC phase is *generated*. These phenomena are quite curious and they could not be observed in the system without chiral imbalance, especially without chemical potential  $\mu_5$ , since at  $\mu_5 = 0$  and at the same values of the basic chemical potentials  $\mu, \nu, \nu_5$ , neither the BSF nor the charged PC phase is present in the system (see Fig. 3 from Ref. [41]).

In part, the phase diagrams in Fig. 6 can also be explained qualitatively at the level of Fermi energies (chemical potentials) for massless left- and right-handed

quarks (3), by employing the pairing arguments. In the region of, for example, charged PC phases of Fig. 6, where  $\mu \approx \nu_5$ , we have from Eq. (3) that  $\mu_{u_R} \approx \nu - \mu_5$  and  $\mu_{d_L} \approx -\nu + \mu_5$ . So one can see that if  $\nu = 0$  (or nonzero but its value should not be close to the value of  $\mu_5$ ), then  $\mu_5 \neq 0$ , both negative and positive, could generate charged PC phase, as it happens in all diagrams of Fig. 6. In a similar way, it is possible to explain qualitatively the presence of the BSF phase in Fig. 6. In the region of  $\nu \approx \nu_5$  and at rather large values of  $\mu_5$  and at zero or nonzero  $\mu \neq 0$  (its value should not just be close to the value of  $\mu_5$ ), the Fermi energies (or chemical potentials) of right-handed  $u$  and  $d$  quarks (3) are  $\mu_{u_R} \approx \mu_{d_R} \approx \mu - \mu_5$ . Then at  $\mu_5 < 0$  [as in Fig. 6(b)] there is a possibility of creation of Cooper pairs (even at  $\mu = 0$ ) of the form  $u_R d_R$ , and their condensation leads to emergence of BSF phase in this case. But at  $\mu = 0$  and  $\mu_5 > 0$  [as in Figs. 6(a) and 6(c)] we have negative values of  $\mu_{u_R}$  and  $\mu_{d_R}$ . It means that in this case there appears Fermi seas (with equal Fermi surfaces) for corresponding antiparticles, i.e., for  $\bar{u}_R$  and  $\bar{d}_R$ . The excitations around these Fermi surfaces can form Cooper  $\bar{u}_R \bar{d}_R$  pairs, and their condensation leads also to the formation of the BSF phase.

Let us now elaborate on the choice of the value of  $\nu_5 = 0.25$  GeV in Fig. 6(a) (instead of  $\nu_5 = 0.4$  GeV). The pattern of the phase structure that we have talked about above was inherent only in the regime of rather large values of chiral isospin imbalance  $\nu_5$ , to be more precise larger than around 0.2 GeV, otherwise the bootlike regions would not emerge and separate from the  $\nu$  and  $\mu$  axis. (The regime of values smaller than 0.2 GeV has been discussed in Sec. IV B.) One can see in Fig. 3(b) that these phases just start to appear at  $\nu_5 = 0.2$  GeV. So the value of  $\nu_5 = 0.25$  GeV was chosen in order to show that the discussed regime works in full fledged mode already at these values. Let us now consider the transitional regime between moderate values of  $\nu_5 < 0.2$  GeV and rather large ones  $\nu_5 > 0.2$  GeV and see how the  $(\mu, \nu)$ -phase diagram depicted in Fig. 3(b) alters, if the chiral imbalance  $\mu_5$  is increased. Now let us consider the transitory region around  $\nu_5 = 0.2$  GeV. Although at  $\nu_5 = 0.2$  GeV and  $\mu_5 = 0$  the regime of moderate values still worked, see Fig. 3(b), when one increases  $\mu_5$  to rather large values, the rather simple picture breaks down and one can see in Fig. 6(c), where the  $(\mu, \nu)$ -phase diagram at  $\mu_5 = 0.5$  GeV and  $\nu_5 = 0.2$  GeV is depicted, that in this case the phase structure is quite rich and complicated. Indeed, there the new regions of charged PC and BSF phases at around  $\mu \approx 0.2$ –0.25 GeV and  $\nu \approx 0.2$ –0.25 GeV appear, as in the case of regime of large  $\nu_5$ . At still larger  $\mu$  and  $\nu$  values the more expected BSF and charged PC phases emerge, as in the case of moderate values  $\nu_5$ . One can see that it is true that in this case the phase diagram is quite involved and rich, and, for example, a lot of first order phase transitions can happen in not so wide range of chemical potentials. If in the case of small or

zero values of isospin imbalance, the baryon density, or  $\mu$ , is increased from small values, first CSB phase takes place, then, if baryon density is increased, charged pion condensation is *triggered* in the system. Comparing Fig. 6(c) with a similar phase diagram of Fig. 3(b) with the same fixed  $\nu_5 = 0.2$  GeV but  $\mu_5 = 0$ , we see that this effect is just due to a nonzero and large value of  $\mu_5$ . Moreover, one could note that in this case the generated value of the charged pion condensate  $\pi_1$  is rather large, see in Fig. 2(c). And then, at still larger values of baryon density, diquark condensation, or BSF phase, is generated [Fig. 2(c)] as in the regime of zero or small  $\mu_5$  and the value of diquark condensate is very considerable. So two first order phase transitions happens in the range of baryon chemical potential  $\mu$  from zero, or even around 0.2 GeV, to 0.3 GeV. By a  $\mathcal{D}_1$ -self-duality of the  $(\mu, \nu)$ -phase diagram of Fig. 6(c), it is clear that at zero or small values of  $\mu$  the isospin chemical potential  $\nu$  is able to generate the BSF phase at nonzero values of  $\mu_5$ . Moreover, applying to the diagrams of Fig. 6 the  $\mathcal{D}_2$ - and  $\mathcal{D}_3$ -dual transformations, it is possible to obtain the  $(\nu, \nu_5)$ - and  $(\mu, \nu_5)$ -phase diagrams of the model at the same fixed values of  $\mu_5$ .

Concluding this section, we would like to note one more interesting property of chiral imbalances in two-color quark matter. Suppose that it is somehow possible to obtain in the system nonzero values of the chiral density of both types and, moreover, to change the values of the corresponding chemical potentials,  $\nu_5$  and  $\mu_5$ . Then practically for arbitrary fixed values of  $\mu$  and  $\nu$  it is possible to get both BSF and charged PC phases, selecting for each of these phenomena the corresponding values of  $\nu_5$  and  $\mu_5$ . The variation of values of  $\nu_5$  and  $\mu_5$  leads to the shifting of the BSF and PC phases in perpendicular directions. (For example, if one increases  $\nu_5$  value, BSF phase occupies the region of larger values of isospin imbalance  $\nu$  at the same  $\mu$  and if one increases  $\mu_5$  BSF phase shifts to the larger baryon density  $\mu$  region with the same value of  $\nu$ .) So the BSF phase, i.e., diquark condensation, to be more precise its place in the phase diagram of dense quark matter with isospin asymmetry, could be controlled by values of chiral imbalances  $\nu_5$  and  $\mu_5$ . And it tells us that diquark condensation phenomenon could be greatly influenced by chiral imbalance of the medium.

Let us summarize in a way and reiterate the following points. In the regime when basic chemical potentials have small or moderate values, chiral chemical potential  $\mu_5$  could only catalyze the phases triggered by basic triple of chemical potentials  $\mu$ ,  $\nu$  and  $\nu_5$ , it is a universal catalyst. But in the regime when basic chemical potentials are rather large, considered in this section, chiral chemical potential  $\mu_5$  can entail rather peculiar symmetry breaking patterns on its own. For example, at  $\mu_5 \neq 0$  (i) one can note that charged PC can emerge in the system even with zero isospin chemical potential, (ii) the diquark condensation can be realized in quark matter with isospin asymmetry,  $\nu \neq 0$ , but zero baryon density,  $\mu = 0$  (see in Fig. 6).

So, the chiral imbalance  $\mu_5$  in various conditions could mimic all chemical potentials possible in the system. For example, in quark matter with zero baryon chemical potential  $\mu_5$  can take a role of  $\mu$  and generate BSF phase in the system. In this sense the feature of chiral imbalance  $\mu_5$  of having the chameleon property manifests itself in this case as well.

## V. SUMMARY AND CONCLUSIONS

In this paper the influence of chiral imbalance  $\mu_5$  on such phenomena of two-color quark matter as chiral symmetry breaking, diquark and charged pion condensations has been scrutinized in the framework of two-color effective NJL model in the mean-field approximation. The influence of other, quark number (or baryon)  $\mu$ , isospin  $\nu$  and chiral isospin  $\nu_5$ , chemical potentials has been investigated in our previous article [41]. While the effect of  $\mu$ ,  $\nu$  and  $\nu_5$  on phase structure, though different, could be grouped together, the influence of  $\mu_5$  is rather peculiar and stands alone from them. The main results of the paper are the following:

- (i) It was shown in the mean-field approximation that at  $\mu_5 \neq 0$  the thermodynamic potential (33) of the model has the same three dual symmetries  $\mathcal{D}_1$  (30),  $\mathcal{D}_2$  and  $\mathcal{D}_3$  (31), found in the case of  $\mu_5 = 0$ . These dualities lead to some fundamental discrete symmetries of the full  $(\mu, \nu, \nu_5, \mu_5)$ -phase diagram of the model, which we also call dual symmetries.
- (ii) Since the duality transformations  $\mathcal{D}_1$ ,  $\mathcal{D}_2$ , and  $\mathcal{D}_3$  do not involve  $\mu_5$ , chiral  $\mu_5$  stands alone from other chemical potentials, baryon, isospin, and chiral isospin chemical potentials, as we call them basic ones, in the sense that at fixed  $\mu_5$  all other chemical potentials are intermingled together by dualities and amalgamated in some  $(\mu, \nu, \nu_5)$  cross section of the full phase diagram of the model. Due to this fact the full  $(\mu, \nu, \nu_5, \mu_5)$ -phase diagram could be envisaged as a foliation of the  $(\mu, \nu, \nu_5)$ -phase portraits along the axis of chiral imbalance  $\mu_5$ . And each  $\mu_5 \neq 0$ -fixed cross section of the full phase diagram, or its  $(\mu, \nu, \nu_5)$ -phase portrait, is highly symmetric to the same extent as at  $\mu_5 = 0$ .
- (iii) This fact entails the number of very interesting implications for the phase structure. Due to it various cross sections of  $(\mu, \nu, \nu_5)$ -phase diagram are self-dual (for example, each  $(\mu, \nu)$ -phase diagram of Figs. 3 and 6 is a  $\mathcal{D}_1$ -self-dual). So it is very easy to analyze it by performing numerical calculations of one of its phase portraits, and then applying to it different duality mappings [e.g., in Fig. 4 the middle and right panels are, respectively,  $\mathcal{D}_2$  and  $\mathcal{D}_3$  conjugated to Fig. 4(a)]. If one varies the chiral imbalance  $\mu_5$ , then the  $(\mu, \nu, \nu_5)$ -phase diagram as a

whole is distorted and transformed, but its property of high symmetry remains intact.

- (iv) The full  $(\mu, \nu, \nu_5, \mu_5)$ -phase structure of the model could be divided into two regimes. In the first one, when basic chemical potentials  $\mu, \nu, \nu_5$  have small or moderate values  $< 0.2$  GeV, the picture is quite frugal in details, but concise and elegant (see in Sec. IV B). The phase diagram has the property that each basic chemical potential is connected by one-to-one correspondence to some phenomenon that it generates, i.e., chiral isospin chemical potential  $\nu_5$  generates CSB, isospin chemical potential  $\nu$  leads to charged PC phenomenon and  $\mu$  entails BSF diquark condensation phenomenon. The whole phase diagram can be sketched in the few lines, the relation between three chemical potentials  $\mu, \nu, \nu_5$  fully defines the phase structure and the largest chemical potential triggers the corresponding phenomenon and hence the corresponding symmetry breaking pattern. While the relation between values of these chemical potentials determine the phase settled in the system, the increase of chiral chemical potential  $\mu_5$  does not meddle in this phase rivalry, it plays the unique role of universal catalyzer, i.e., it catalyzes any of these phases picked by basic chemical potentials and drastically enhances the value of the corresponding condensate.

So the chiral chemical potential  $\mu_5$  stands alone from the other chemical potentials not only in terms of dual properties. Its influence on the phase diagram in this regime is drastically different to other (basic) chemical potentials. Chiral chemical potential assumes the property of the largest basic chemical potential (that determines the phase) and catalyzes the corresponding phenomenon even further. So it could mimic the effect of other chemical potentials. Especially clear, this is seen in the case where there is only one chemical potential besides  $\mu_5$ . In this scenario the phase diagram is very symmetric and chiral chemical potential  $\mu_5$  takes a role of this chemical potential and, mimicking it, catalyzes the corresponding phenomenon. This property was called the chameleon one by analogy with chameleon and its ability to assume the color of the environment in which it is placed.

- (v) In the second regime of rather large values of basic chemical potentials  $\mu, \nu, \nu_5$  (at least when two of them are larger than 0.2 GeV), the phase diagram is much more involved and has rich structure, especially if there are all three nonzero basic chemical potentials, see, e.g., in Fig. 6. In this regime the chiral imbalance  $\mu_5$  is not just a universal catalyst for any pattern of symmetry breaking in the system. It is able to induce some dynamical symmetry breaking on its own and trigger rather peculiar phases in the

system. For example, diquark condensation at zero baryon chemical potential  $\mu = 0$ , which is rather peculiar and could not occur without  $\mu_5$ .

In this case, as well depending on the situation, chiral chemical potential  $\mu_5$  can pretend to be any basic chemical potential  $\mu, \nu, \nu_5$ . For example,  $\mu_5$  can assume the role of baryon chemical potential  $\mu$  and generate the diquark condensation. Also  $\mu_5$  can mimic either isospin chemical potential  $\nu$  and trigger charged PC, or chiral isospin chemical potential  $\nu_5$  and be a reason of chiral symmetry breaking. And in this sense the statement that the chiral imbalance has a chameleon nature is supported once again.

- (vi) Chameleon nature of chiral imbalance is a rather universal phenomenon and it can be observed in both regimes, as for small and moderate values of basic chemical potentials, as well as for rather large ones. The unique role of  $\mu_5$  as a universal catalyzer is also one of manifestation of this effect. Chiral imbalance  $\mu_5$  can promote all phenomena happening in two-color quark matter, this property is based on the fact that at fixed  $\mu_5$  the  $(\mu, \nu, \nu_5)$ -phase diagram of the two-color NJL model is highly symmetric due to dualities (see in Sec. III). All these leads to the fact that, using duality mappings, one can shuffle the facets of the  $(\mu, \nu, \nu_5)$ -phase diagram. So if  $\mu_5$  promotes some phenomenon, it could promote two others in the dually conjugated sectors of the  $(\mu, \nu, \nu_5)$ -phase diagram. So the influence of chiral chemical potential  $\mu_5$  on the phase structure is highly constrained by dualities, its chameleon nature is inevitable consequence of dual properties of the phase diagram.

In the presence of only one nonzero chemical potential  $\mu$ , the results of our paper can be compared with lattice approach to 2-color QCD (see, e.g., Ref. [10]). In this case, two different approaches, NJL and lattice one, to 2-color QCD with only  $\mu \neq 0$  predict a qualitatively identical phase structure of this model in the region of not very large values of  $\mu$ . Extrapolating this result to the case of 2-color QCD with several chemical potentials, we can conclude that our results quite adequately represent the phase structure of massless 2-color QCD in the region of intermediate values of basic, i.e.,  $\mu, \nu, \nu_5$ , chemical potentials, say, lower than  $\Lambda \approx 0.65$  GeV.

As for the interval of  $\mu_5$  values, for which the properties of the 2-color NJL model, obtained in our consideration, can be extended (at least at a qualitative level) to the cases of both two- and three-color QCD, we predict a more narrow interval, namely  $|\mu_5| < 500$  GeV (or even smaller). The first reason is that the UV cutoff  $\Lambda$ , as it was shown in Ref. [46], cuts effectively important degrees of freedom of the system and can lead to the wrong result, if  $\mu_5$  is near the cutoff. The second one is that the predictions of any NJL

model depend to a large extent on the regularization scheme. For example, in our paper the sharp cutoff scheme is used, for simplicity. And in this case the chiral condensate is enhanced by  $\mu_5$  at rather small interval  $\mu_5 \lesssim 0.4$  GeV [see in Fig. 2(a)]. However, there is a more sophisticated, the so-called medium separation scheme, regularization approach to NJL model. In the case with single  $\mu_5$ , it supplies an increasing of chiral condensate over a much larger range of  $\mu_5$  [49]. And just the last result is in agreement with first-principal lattice study of the 2-color QCD with only  $\mu_5 \neq 0$  [47]. Due to technical difficulties that arise in the case of several chemical potentials, the medium separation regularization scheme was not used in our present investigation. Nevertheless, we guess that the

phase diagram of the 2-color NJL model considered in our paper, even within the framework of the simplest regularization scheme, shows all the elegance inherent in the phase structure of a 2-color QCD with different densities and clarifies the properties of the  $\mu_5$  chiral imbalance. And its effect on the phase structure, which may turn out to be universal and inherent as well, or have some common features, with the 3-color QCD.

## ACKNOWLEDGMENTS

The work by R. N. Z. was supported by the Foundation for the Advancement of Theoretical Physics and Mathematics BASIS.

- 
- [1] K. Fukushima and T. Hatsuda, *Rep. Prog. Phys.* **74**, 014001 (2011); M. G. Alford, A. Schmitt, K. Rajagopal, and T. Schafer, *Rev. Mod. Phys.* **80**, 1455 (2008).
- [2] Y. Nambu and G. Jona-Lasinio, *Phys. Rev.* **122**, 345 (1961).
- [3] S. P. Klevansky, *Rev. Mod. Phys.* **64**, 649 (1992); D. Ebert, H. Reinhardt, and M. K. Volkov, *Prog. Part. Nucl. Phys.* **33**, 1 (1994); T. Inagaki, T. Muta, and S. D. Odintsov, *Prog. Theor. Phys. Suppl.* **127**, 93 (1997); A. A. Garibli, R. G. Jafarov, and V. E. Rochev, *Symmetry* **11**, 668 (2019).
- [4] M. Buballa, *Phys. Rep.* **407**, 205 (2005).
- [5] S. Muroya, A. Nakamura, C. Nonaka, and T. Takaishi, *Prog. Theor. Phys.* **110**, 615 (2003).
- [6] K. Splittorff, D. T. Son, and M. A. Stephanov, *Phys. Rev. D* **64**, 016003 (2001).
- [7] J. B. Kogut, M. A. Stephanov, and D. Toublan, *Phys. Lett. B* **464**, 183 (1999); J. B. Kogut, M. A. Stephanov, D. Toublan, J. J. M. Verbaarschot, and A. Zhitnitsky, *Nucl. Phys.* **B582**, 477 (2000).
- [8] C. Ratti and W. Weise, *Phys. Rev. D* **70**, 054013 (2004).
- [9] S. Hands, I. Montvay, L. Scorzato, and J. Skullerud, *Eur. Phys. J. C* **22**, 451 (2001).
- [10] V. V. Braguta, E. M. Ilgenfritz, A. Y. Kotov, A. V. Molochkov, and A. A. Nikolaev, *Phys. Rev. D* **94**, 114510 (2016).
- [11] K. Iida and E. Itou, [arXiv:2207.01253](https://arxiv.org/abs/2207.01253).
- [12] D. C. Duarte, P. G. Allen, R. L. S. Farias, P. H. A. Manso, R. O. Ramos, and N. N. Scoccola, *Phys. Rev. D* **93**, 025017 (2016).
- [13] J. O. Andersen and A. A. Cruz, *Phys. Rev. D* **88**, 025016 (2013).
- [14] T. Brauner, K. Fukushima, and Y. Hidaka, *Phys. Rev. D* **80**, 074035 (2009); **81**, 119904(E) (2010).
- [15] J. O. Andersen and T. Brauner, *Phys. Rev. D* **81**, 096004 (2010).
- [16] S. Imai, H. Toki, and W. Weise, *Nucl. Phys.* **A913**, 71 (2013).
- [17] P. Adhikari, S. B. Beleznyay, and M. Mannarelli, *Eur. Phys. J. C* **78**, 441 (2018); P. Adhikari and H. Nguyen, *Eur. Phys. J. Plus* **135**, 789 (2020).
- [18] J. Chao, *Chin. Phys. C* **44**, 034108 (2020).
- [19] V. G. Bornyakov, V. V. Braguta, A. A. Nikolaev, and R. N. Rogalyov, *Phys. Rev. D* **102**, 114511 (2020).
- [20] T. Khunjua, K. Klimenko, and R. Zhokhov, *Phys. Part. Nucl.* **53**, 461 (2022).
- [21] T. Furusawa, Y. Tanizaki, and E. Itou, *Phys. Rev. Research* **2**, 033253 (2020).
- [22] S. Datta, S. Gupta, and R. Sharma, *Indian J. Phys.* **95**, 1623 (2021).
- [23] M. A. Metlitski and A. R. Zhitnitsky, *Phys. Rev. D* **72**, 045011 (2005).
- [24] K. Fukushima, D. E. Kharzeev, and H. J. Warringa, *Phys. Rev. D* **78**, 074033 (2008).
- [25] K. Fukushima, D. E. Kharzeev, and H. J. Warringa, *Phys. Rev. Lett.* **104**, 212001 (2010).
- [26] K. Fukushima, D. E. Kharzeev, and H. J. Warringa, *Nucl. Phys.* **A836**, 311 (2010).
- [27] D. E. Kharzeev, *Prog. Part. Nucl. Phys.* **75**, 133 (2014).
- [28] M. N. Chernodub and A. S. Nedelin, *Phys. Rev. D* **83**, 105008 (2011).
- [29] T. G. Khunjua, K. G. Klimenko, and R. N. Zhokhov, *Eur. Phys. J. C* **79**, 151 (2019); *J. High Energy Phys.* **06** (2019) 006; *J. Phys.* **1390**, 012015 (2019).
- [30] L. He, M. Jin, and P. Zhuang, *Phys. Rev. D* **71**, 116001 (2005); D. Ebert and K. G. Klimenko, *J. Phys. G* **32**, 599 (2006); *Eur. Phys. J. C* **46**, 771 (2006); C.-f. Mu, L.-y. He, and Y.-x. Liu, *Phys. Rev. D* **82**, 056006 (2010).
- [31] H. Abuki, R. Anglani, R. Gatto, G. Nardulli, and M. Ruggieri, *Phys. Rev. D* **78**, 034034 (2008); H. Abuki, R. Anglani, R. Gatto, M. Pellicoro, and M. Ruggieri, *Phys. Rev. D* **79**, 034032 (2009); R. Anglani, *Acta Phys. Pol. B Proc. Suppl.* **3**, 735 (2010).
- [32] J. O. Andersen and T. Brauner, *Phys. Rev. D* **78**, 014030 (2008); J. O. Andersen and L. Kyllingstad, *J. Phys. G* **37**, 015003 (2009); Y. Jiang, K. Ren, T. Xia, and P. Zhuang, *Eur. Phys. J. C* **71**, 1822 (2011); A. Folkestad and J. O. Andersen, *Phys. Rev. D* **99**, 054006 (2019); P. Adhikari, J. O. Andersen, and P. Kneschke, *Phys. Rev. D* **98**, 074016

- (2018); *Eur. Phys. J. C* **79**, 874 (2019); J. O. Andersen, P. Adhikari, and P. Kneschke, *Proc. Sci., Confinement2018* (2019) 197 [arXiv:1810.00419].
- [33] D. Ebert, T. G. Khunjua, K. G. Klimenko, and V. C. Zhukovsky, *Int. J. Mod. Phys. A* **27**, 1250162 (2012); N. V. Gubina, K. G. Klimenko, S. G. Kurbanov, and V. C. Zhukovsky, *Phys. Rev. D* **86**, 085011 (2012).
- [34] A. Mammarella and M. Mannarelli, *Phys. Rev. D* **92**, 085025 (2015); S. Carignano, L. Lepori, A. Mammarella, M. Mannarelli, and G. Pagliaroli, *Eur. Phys. J. A* **53**, 35 (2017); M. Mannarelli, *Particles* **2**, 411 (2019).
- [35] J. O. Andersen and P. Kneschke, arXiv:1807.08951; B. B. Brandt, G. Endrodi, E. S. Fraga, M. Hippert, J. Schaffner-Bielich, and S. Schmalzbauer, *Phys. Rev. D* **98**, 094510 (2018).
- [36] S. S. Avancini, A. Bandyopadhyay, D. C. Duarte, and R. L. S. Farias, *Phys. Rev. D* **100**, 116002 (2019); B. S. Lopes, S. S. Avancini, A. Bandyopadhyay, D. C. Duarte, and R. L. S. Farias, *Phys. Rev. D* **103**, 076023 (2021).
- [37] T. G. Khunjua, K. G. Klimenko, and R. N. Zhokhov, *Symmetry* **11**, 778 (2019); *Particles* **3**, 62 (2020).
- [38] T. G. Khunjua, K. G. Klimenko, and R. N. Zhokhov, *Phys. Rev. D* **97**, 054036 (2018).
- [39] T. Khunjua, K. Klimenko, and R. Zhokhov, *EPJ Web Conf.* **191**, 05015 (2018); *Phys. Rev. D* **98**, 054030 (2018); **100**, 034009 (2019); *Moscow Univ. Phys. Bull.* **74**, 473 (2019).
- [40] I. A. Shovkovy, *Found. Phys.* **35**, 1309 (2005); M. Huang, *Int. J. Mod. Phys. E* **14**, 675 (2005); K. G. Klimenko and D. Ebert, *Teor. Mat. Fiz.* **150**, 95 (2007) [*Theor. Math. Phys.* **150**, 82 (2007)]; M. G. Alford, A. Schmitt, K. Rajagopal, and T. Schäfer, *Rev. Mod. Phys.* **80**, 1455 (2008); E. J. Ferrer and V. de la Incera, *Lect. Notes Phys.* **871**, 399 (2013).
- [41] T. G. Khunjua, K. G. Klimenko, and R. N. Zhokhov, *J. High Energy Phys.* **06** (2020) 148.
- [42] M. Ruggieri, G. X. Peng, and M. Chernodub, *EPJ Web Conf.* **129**, 00037 (2016); M. Ruggieri and G. X. Peng, *Phys. Rev. D* **93**, 094021 (2016).
- [43] R. Gatto and M. Ruggieri, *Phys. Rev. D* **85**, 054013 (2012); L. Yu, H. Liu, and M. Huang, *Phys. Rev. D* **90**, 074009 (2014); **94**, 014026 (2016); M. Ruggieri and G. X. Peng, *J. Phys. G* **43**, 125101 (2016); A. A. Andrianov, V. A. Andrianov, and D. Espriu, *Particles* **3**, 15 (2020); D. Espriu, A. G. Nicola, and A. Vioque-Rodriguez, *J. High Energy Phys.* **06** (2020) 062.
- [44] M. Ruggieri, M. N. Chernodub, and Z. Y. Lu, *Phys. Rev. D* **102**, 014031 (2020).
- [45] G. Cao and P. Zhuang, *Phys. Rev. D* **92**, 105030 (2015).
- [46] V. V. Braguta and A. Y. Kotov, *Phys. Rev. D* **93**, 105025 (2016).
- [47] V. V. Braguta, V. A. Goy, E.-M. Ilgenfritz, A. Y. Kotov, A. V. Molochkov, M. Muller-Preussker, and B. Petersson, *J. High Energy Phys.* **06** (2015) 094.
- [48] V. V. Braguta, E. M. Ilgenfritz, A. Y. Kotov, B. Petersson, and S. A. Skinderev, *Phys. Rev. D* **93**, 034509 (2016); N. Y. Astrakhantsev, V. V. Braguta, A. Y. Kotov, and A. A. Nikolaev, *Eur. Phys. J. A* **57**, 15 (2021); V. V. Braguta, M. I. Katsnelson, A. Y. Kotov, and A. M. Trunin, *Phys. Rev. B* **100**, 085117 (2019).
- [49] R. L. S. Farias, D. C. Duarte, G. Krein, and R. O. Ramos, *Phys. Rev. D* **94**, 074011 (2016).